The Arabidopsis Transcription Factor BRASSINOSTEROID INSENSITIVE1-ETHYL METHANESULFONATE-SUPPRESSOR1 Is a Direct Substrate of MITOGEN-ACTIVATED PROTEIN KINASE6 and Regulates Immunity[1]

Sining Kang, Fan Yang, Lin Li, Huamin Chen, She Chen, and Jie Zhang*

State Key Laboratory of Plant Genomics, Institute of Microbiology, Chinese Academy of Sciences, Beijing 100101, China (S.K., F.Y., J.Z.); University of Chinese Academy of Sciences, Beijing 100049, China (F.Y.); National Institute of Biological Sciences, Zhongguancun Life Science Park, Beijing 102206, China (L.L., S.C.); and State Key Laboratory for Biology of Plant Diseases and Insect Pests, Institute of Plant Protection, Chinese Academy of Agricultural Sciences, Beijing 100193, China (H.C.)

Pathogen-associated molecular patterns (PAMPs) are recognized by plant pattern recognition receptors to activate PAMP-triggered immunity (PTI). Mitogen-activated protein kinases (MAPKs), as well as other cytoplasmic kinases, integrate upstream immune signals and, in turn, dissect PTI signaling via different substrates to regulate defense responses. However, only a few direct substrates of these signaling kinases have been identified. Here, we show that PAMP perception enhances phosphorylation of BRASSINOSTEROID INSENSITIVE1-ETHYL METHANESULFONATE-SUPPRESSOR1 (BES1), a transcription factor involved in brassinosteroid (BR) signaling pathway, through pathogen-induced MAPKs in Arabidopsis (*Arabidopsis thaliana*). BES1 interacts with MITOGEN-ACTIVATED PROTEIN KINASE6 (MPK6) and is phosphorylated by MPK6. *bes1* loss-of-function mutants display compromised resistance to bacterial pathogen *Pseudomonas syringae* pv *tomato* DC3000. BES1 S286A/S137A double mutation ($BES1^{SSAA}$) impairs PAMP-induced phosphorylation and fails to restore bacterial resistance in *bes1* mutant, indicating a positive role of BES1 phosphorylation in plant immunity. BES1 is phosphorylated by glycogen synthase kinase3 (GSK3)-like kinase BR-insensitive2 (BIN2), a negative regulator of BR signaling. BR perception inhibits BIN2 activity, allowing dephosphorylation of BES1 to regulate plant development. However, $BES1^{SSAA}$ does not affect BR-mediated plant growth, suggesting differential residue requirements for the modulation of BES1 phosphorylation in PTI and BR signaling. Our study identifies BES1 as a unique direct substrate of MPK6 in PTI signaling. This finding reveals MAPK-mediated BES1 phosphorylation as another BES1 modulation mechanism in plant cell signaling, in addition to GSK3-like kinase-mediated BES1 phosphorylation and F box protein-mediated BES1 degradation.

Plants are challenged with pathogenic microbes during their whole life cycle. Conserved molecular patterns derived from bacteria and fungi are recognized by plant cell surface-localized pattern recognition receptors (PRRs) to activate pathogen-associated molecular pattern (PAMP)-triggered immunity (PTI; Schwessinger and Zipfel, 2008). Several receptor kinases such as flagellin sensing2 (FLS2) and elongation factor thermo unstable (EF-Tu) receptor have been identified as PRRs recognizing bacterial flagellin and EF-Tu, respectively (Gómez-Gómez and Boller, 2000; Chinchilla et al., 2006; Zipfel et al., 2006). PTI confers broad and durable resistance against microbial pathogens. However, PTI signal transduction mechanisms remain not well understood. A few important cytoplasmic kinases, including mitogen-activated protein kinases (MAPKs), calcium-dependent protein kinases, and receptor-like cytoplasmic kinases, have been identified to integrate and amplify immune signals from activated PRRs (Veronese et al., 2006; Pitzschke et al., 2009; Boudsocq et al., 2010; Lu et al., 2010; Zhang et al., 2010) and in turn regulate downstream defense responses. The direct substrates for PTI signaling cytoplasmic kinases in PTI remain not well characterized.

In FLS2-mediated signaling pathway, *botrytis*-induced kinase1 (BIK1) and AVRPPHB SUSCEPTIBLE1-like1 (PBL1) associate with FLS2 prior to flagellin perception (Lu et al., 2010; Zhang et al., 2010). Binding of flagellar N-terminal peptide flg22 to FLS2 triggers recruitment of BRASSINOSTEROID-INSENSITIVE1-associated receptor kinase1 (BAK1) to FLS2 (Gómez-Gómez et al., 1999; Chinchilla et al., 2006, 2007; Heese et al., 2007; Sun et al., 2013) and also induces BIK1 phosphorylation and its dissociation from FLS2 (Lu et al., 2010; Zhang et al., 2010). Plant U-box (PUB) proteins PUB12 and PUB13

[1] This work was supported by the Strategic Priority Research Program of the Chinese Academy of Sciences (grant no. XDB11020600) and the Chinese Natural Science Foundation (grant no. 31300234).

* Address correspondence to zhangjie@im.ac.cn.

The author responsible for distribution of materials integral to the findings presented in this article in accordance with the policy described in the Instructions for Authors (www.plantphysiol.org) is: Jie Zhang (zhangjie@im.ac.cn).

www.plantphysiol.org/cgi/doi/10.1104/pp.114.250985

ubiquitinate FLS2 for degradation to attenuate PTI (Lu et al., 2011). Most recently, Arabidopsis respiratory burst oxidase homolog D (AtrbohD) has been reported to act as a direct substrate of BIK1 and contribute to BIK1-regulated stomatal defense (Kadota et al., 2014; Li et al., 2014). Downstream of PRR activation, both MITOGEN-ACTIVATED PROTEIN KINASE KINASE4 (MKK4)/MKK5-MITOGEN-ACTIVATED PROTEIN KINASE3 (MPK3)/MPK6 cascades and MITOGEN-ACTIVATED PROTEIN KINASE KINASE KINASE1 (MEKK1)-MKK1/MKK2-MPK4 cascades are activated (Pitzschke et al., 2009). Mitogen-activated protein kinase4 substrate1 (MKS1) is a direct substrate of MPK4 that cooperates with WRKY33 to regulate target gene expression (Andreasson et al., 2005). 1-Aminocyclopropane-1-carboxylic acid synthase ACS2 and ACS6 are substrates of MPK3/MPK6 and regulate ethylene production in response to pathogen invasion (Liu and Zhang, 2004; Han et al., 2010; Li et al., 2012). AtPHOS32 (for phosphorylated protein with an apparent molecular mass of 32 kDa), ethylene response factor104 (AtERF104), and VIRULENCE PROTEIN E2-interacting protein1 (VIP1) are the only identified substrates of MPK6 and/or MPK3 in PTI, whereas their biological roles in PTI remain to be further characterized (Peck et al., 2001; Djamei et al., 2007; Merkouropoulos et al., 2008; Bethke et al., 2009). Identification of additional MAPK substrates is critical for uncovering the molecular mechanism of PTI signaling dissection.

Immune signals integrated by PTI signaling kinases induce the transcriptional reprogramming of a large number of defense-related genes. Histone methylation is a key epigenetic mechanism that regulates chromatin structure and gene expression. Thus, histone-modifying enzymes and related transcription regulators are candidate substrates for PTI signaling kinases. Several histone methyltransferases have been reported to regulate plant resistance against bacterial and fungal pathogens (Alvarez-Venegas et al., 2007; Berr et al., 2010). However, whether histone demethylase (HDM) is involved in plant immunity remains uncertain. BRASSINOSTEROID INSENSITIVE1-ETHYL METHANESULFONATE-SUPPRESSOR1 (BES1) is a major transcription factor in brassinosteroid (BR)-mediated signaling pathway. BR regulates BES1 activity through phosphorylation and dephosphorylation to control BR-responsive gene expression (Yin et al., 2002, 2005). BES1 has also been reported to recruit HDM EARLY FLOWERING6 (ELF6) and RELATIVE OF ELF6 to regulate BR-responsive gene expression (Yu et al., 2008). In addition, BES1 also participates in strigolactone (SL) signaling via F box protein-mediated degradation to control shoot branching (Wang et al., 2013).

In this study, we uncover a unique function of BES1 in plant immunity. We demonstrate that perception of flg22, a bacterial PAMP, enhances phosphorylation of BES1. This enhanced phosphorylation is prevented by the expression of either a bacterial MAPK inhibitor, hypersensitive response and pathogenicity-dependent outer protein AI1 (HopAI1), or the $MKK5^{K99M}$ dominant negative mutant, indicating a MAPK-dependent BES1 phosphorylation triggered by PAMP perception. Further analyses prove that BES1 interacts with MPK6 and is phosphorylated by MPK6 in vitro. *bes1* mutants are compromised in bacterial resistance against *Pseudomonas syringae* pv *tomato* DC3000 (*Pst* DC3000). Furthermore, BES1 S286A/S137A double mutation ($BES1^{SSAA}$) impairing PAMP-induced phosphorylation fails to restore bacterial resistance in *bes1* mutant but does not affect BR-mediated plant growth. Taken together, these data demonstrate BES1 as a direct substrate of MPK6 in PTI signaling and indicate differential modulation of a common transcription factor targeted by distinct signaling proteins in hormone and immunity signaling in plants.

RESULTS

BES1 Contributes to Plant Immunity to *P. syringae*

To investigate the role of histone demethylation in plant immune regulation, we carried out a reverse genetic screen to identify HDMs as well as HDM-bound transcription factors involved in Arabidopsis (*Arabidopsis thaliana*) bacterial resistance. Transfer DNA insertion lines of HDMs and HDM-bound transcription factors were inoculated with *P. syringae* strain *Pst* DC3000, and then in planta bacterial growth was assessed in mutant plants. Transfer DNA insertion mutants *bes1-1* (He et al., 2005) and *bes1-2* (Supplemental Fig. S1A), which supported more bacterial growth of *Pst* DC3000 (Fig. 1A) and developed more severe disease symptoms than ecotype Columbia (Col-0) wild-type plants (Supplemental Fig. S1B), were isolated. Quantitative reverse transcription-PCR data showed that *BES1* expression in *bes1-1* and *bes1-2* mutants is significantly decreased compared with that in wild-type plants (Supplemental Fig. S1C). To study whether *BES1* regulates the expression of PTI-responsive genes, *bes1* mutants were treated with flg22 and the induction of PTI-responsive genes was measured. A reduction in *WRKY22* and *FLG22-INDUCED RECEPTOR-LIKE KINASE1* (*FRK1*) induction by flg22 was detected in *bes1* mutants compared with wild-type plants (Fig. 1, B and C). Compromised bacterial resistance and defensive gene induction in *bes1* mutants indicate that BES1 positively regulates plant immunity against bacterial pathogens.

Flagellin Perception Enhances BES1 Phosphorylation

BES1 activity is regulated by phosphorylation and dephosphorylation in BR signaling pathway. In the absence of BR, BES1 is phosphorylated by the upstream glycogen synthase kinase3 (GSK3)-like kinase BR-insensitive2 (BIN2) and retained in the cytoplasm (Yin et al., 2002, 2005; Ryu et al., 2010). Perception of BR triggers dephosphorylation of BES1 and results in its accumulation in the nucleus to direct expression of BR-responsive genes (Yin et al., 2002; Ryu et al., 2010). We then speculated a modulation of BES1 phosphorylation by PAMP perception. *BES1* native promoter-driven *BES1* tagged with a FLAG epitope (*BES1*::*BES1-FLAG*)

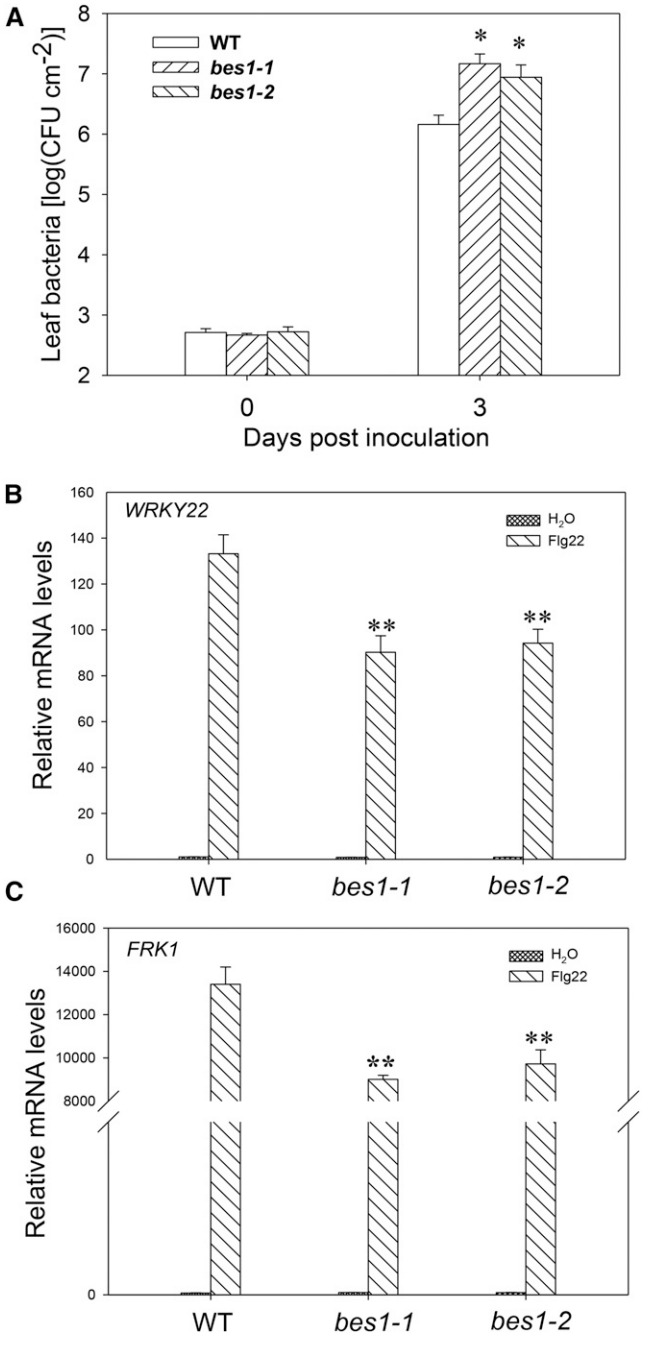

Figure 1. BES1 contributes to plant immunity. A, Growth of *Pst* DC3000 in wild-type (WT; Col-0), *bes1-1*, and *bes1-2* plants. Wild-type or mutant plants were infiltrated with 10^5 cfu mL^{-1} *Pst* DC3000, and leaf bacterial population was determined at the indicated times. The results shown are representative of three independent experiments. An asterisk indicates significant difference at $P < 0.05$. B, *BES1* is required for full induction of *WRKY22* by Flg22. C, *BES1* is required for full induction of *FRK1* by Flg22. Five-week-old wild-type or *bes1* mutant plants were infiltrated with or without 500 nM flg22 for 3 h. Total RNA was extracted and used for reverse transcription. Real-time PCR was performed following standard protocols. Values are normalized to *TUBLIN* control and are presented as relative to the value of water-treated wild-type plants. Error bars indicate SD of three technical repeats. Asterisks indicate significant difference to the flg22-treated wild type at $P < 0.01$. Similar results were observed in three independent biological repeats.

transgenic plants were constructed and used to study BES1 phosphorylation in response to PAMP treatment (Supplemental Materials and Methods S1). In untreated plants, both faster-migrating and slower-migrating forms of BES1 can be detected, as previously reported (Yin et al., 2002; Albrecht et al., 2012). We found that flg22 treatment resulted in the appearance of an intermediate-migrating BES1 in *BES1*::*BES1-FLAG* transgenic plants (Fig. 2, A and B, asterisk indicated). The appearance of this intermediate-migrating BES1 was removed by the treatment of λ protein phosphatase (PPase), indicating an elevated phosphorylation of BES1 upon flg22 stimulation (Fig. 2A). Epibrassinolide (EpiBL) has been shown to trigger dephosphorylation of BES1 (Yin et al., 2002; Albrecht et al., 2012). We wondered whether flg22 is able to resume

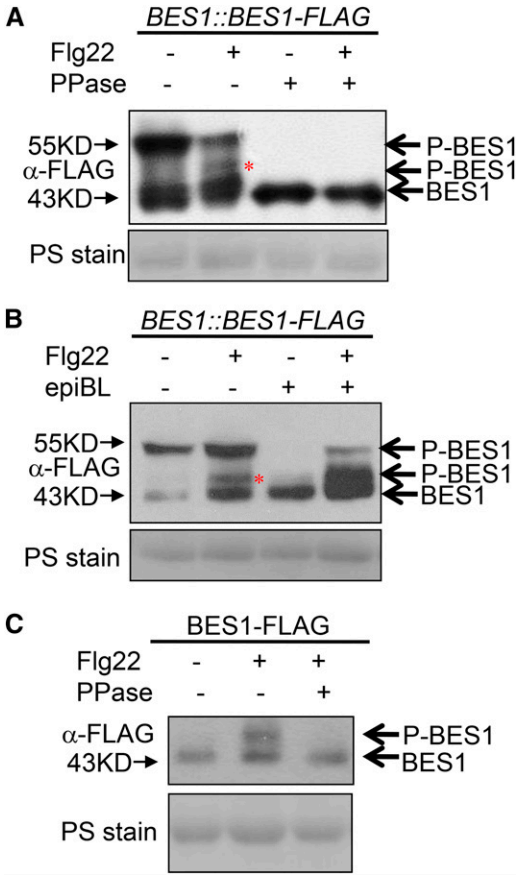

Figure 2. Flg22 enhances BES1 phosphorylation. A, Flg22 induces BES1 phosphorylation in plants. *BES1*::*BES1-FLAG* transgenic plants were treated with water or 1 μM flg22 for 5 min, and total protein extracted from leaves was treated with or without PPase as indicated. B, Flg22 induces BES1 rephosphorylation after BL pretreatment in plants. *BES1*::*BES1-FLAG* transgenic plants were pretreated with or without 1 μM epiBL as indicated for 1 h, followed by 1 μM flg22 treatment for 5 min. C, Flg22 induces BES1 phosphorylation in protoplasts. Col-0 protoplasts were transfected with *35S*::*BES1-FLAG*, treated with or without 1 μM flg22. Total protein extracted from protoplasts was treated with or without PPase as indicated. Protein samples were separated by SDS-PAGE and subjected to anti-FLAG immunoblot. Ponceau S (PS) staining of the filter indicates loading of the protein.

phosphorylation of dephosphorylated BES1 in epiBL-pretreated plants. Hence, *BES1*::*BES1-FLAG* plants were pretreated with epiBL to eliminate basal level of phosphorylated BES1 and then treated with flg22. The following flg22 treatment clearly resumed phosphorylation of BES1 (Fig. 2B). This result confirms an elevated BES1 phosphorylation triggered by PAMP perception in plants. In agreement with the results from *BES1*::*BES1-FLAG* transgenic plants, flg22 treatment resulted in a slower mobility shift of BES1 in Arabidopsis protoplasts transfected with *35S*::*BES1-FLAG* when compared with water treatment (Fig. 2C). Similar to that in transgenic plants, the mobility shift was removed by treatment of λ PPase (Fig. 2C), indicating an elevated phosphorylation of transiently expressed BES1 upon flg22 stimulation in protoplast. In addition to flg22, Crab shell chitin and elf18 (an *N*-acetylated peptide comprising the first 18 amino acids of EF-Tu) treatments also induced phosphorylation of BES1 (Supplemental Fig. S2). Taken together, the above results proved an elevated phosphorylation of BES1 triggered by PAMP perception in plants.

BES1 Phosphorylation Induced by flg22 Occurs Downstream of MAPK Activation

PAMP perception triggers both activation of MAPK cascades and phosphorylation of BIK1/PBL1, which are likely to act in two branches to regulate downstream responses (Zhang and Zhou, 2010). To determine the causal relationship between BES1 phosphorylation and other early signaling events, we next examined BES1 phosphorylation induced by flg22 in *bik1/pbl1* double mutant, because *BIK1* and *PBL1* function redundantly in PTI signaling. We observed that flg22 induced phosphorylation of BES1 in the *bik1/pbl1* double mutant (Fig. 3A). We previously reported that $BIK1^{K105E}$, an ATP binding site mutant of BIK1, has a dominant-negative effect on PTI signaling (Zhang et al., 2010). Hence, we further examined whether BES1 phosphorylation induced by flg22 could be prevented by $BIK1^{K105E}$. Consistent with the result of *bik1/pbl1* double mutant, overexpression of $BIK1^{K105E}$ did not prevent flg22-induced BES1 phosphorylation (Fig. 3B), suggesting that BIK1 and PBL1 are not required for BES1 phosphorylation induced by flg22.

Next, we checked MAPK activation induced by flg22 in *bes1* mutants. Extent of MAPK activation induced by flg22 was comparable in *bes1-1*, *bes1-2*, and wild-type plants (Supplemental Fig. S3), suggesting that flg22-induced BES1 phosphorylation is likely to be either downstream or independent of MAPK activation. This promoted us to test whether MAPK activation is required for BES1 phosphorylation induced by flg22. In a previous study, we identified the unique phospho-Thr lyase activity of a *P. syringae* effector HopAI1 toward MPKs (Zhang et al., 2007, 2012), leading to permanent inactivation of MPK3, MPK6, and MPK4. Thus, HopAI1 was used as a bacterial inhibitor to block MAPK activation by flg22 in vivo. We observed that BES1 phosphorylation induced by flg22 was abolished in the presence of HopAI1 (Fig. 3C). $MKK5^{K99M}$ acts as a dominant negative mutant that partially blocks MAPK activation and downstream PTI signaling (Asai et al., 2002). Coexpression of $MKK5^{K99M}$ with BES1 also inhibited BES1 phosphorylation induced by flg22 (Fig. 3D). These results suggested that flg22-induced BES1 phosphorylation occurs downstream of MAPK activation.

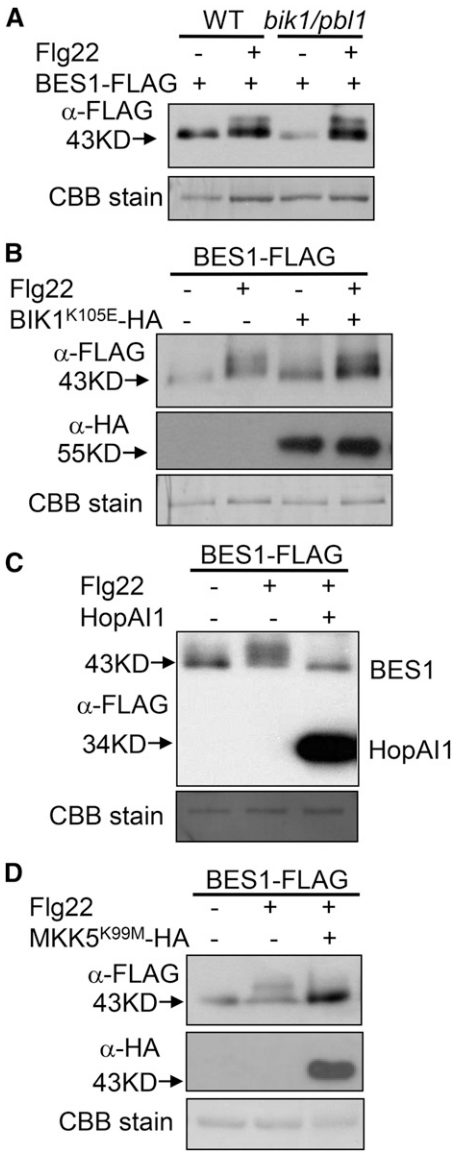

Figure 3. BES1 phosphorylation induced by flg22 occurs downstream of MAPK activation. A, *BIK1* and *PBL1* are not required for BES1 phosphorylation induced by flg22. B, $BIK1^{K105E}$ does not prevent BES1 phosphorylation induced by flg22. C, BES1 phosphorylation induced by flg22 is prevented by HopAI1. D, BES1 phosphorylation induced by flg22 is partially blocked by $MKK5^{K99M}$. Protoplasts isolated from wild-type (WT) or mutant plants were transfected with *35S*::*BES1-FLAG* or together with *35S*::*$BIK1^{K105E}$-hemagglutinin* (*HA*), *35S*::*HopAI1-FLAG*, or *35S*::*$MKK5^{K99M}$-HA* as indicated, treated with or without 1 μM flg22 for 5 min. Protein samples were separated by SDS-PAGE and subjected to anti-FLAG immunoblot. Coomassie Brilliant Blue (CBB) staining of the filter indicates loading of the protein.

MEKK1-MKK1/MKK2-MPK4 and MKK4/MKK5-MPK3/MPK6 constitute two MAPK cascade branches in PTI signaling. To determine whether MEKK1-MKK1/MKK2-MPK4 branch is responsible for BES1 phosphorylation, the effect of *MPK4* or *MKK1/MKK2* mutation on flg22-induced BES1 phosphorylation was examined. *mpk4* and *mkk1/mkk2* mutant displayed dwarf and autoimmune phenotype (Petersen et al., 2000). Mutation of *SUPPRESSOR OF MKK1 MKK2* (*SUMM2*), a resistance gene that guards the MEKK1-MKK1/MKK2-MPK4 cascade, is able to suppress the autoimmune phenotype of *mpk4* and *mkk1/mkk2* mutant (Zhang et al., 2012). Thus, BES1 phosphorylation induced by flg22 was examined in *mpk4/summ2* and *mkk1/mkk2/summ2* mutants. As shown in Supplemental Figure S4, A and B, flg22 could induce BES1 phosphorylation in both *mpk4/summ2* double mutant and *mkk1/mkk2/summ2* triple mutant, indicating that mutation of *MPK4* or *MKK1/MKK2* is not sufficient to prevent BES1 phosphorylation induced by flg22. Expression of $MKK5^{DD}$, a constitutive active form of MKK5, has been shown to activate MPK3/MPK6 in Arabidopsis protoplasts (Asai et al., 2002). BES-FLAG was then coexpressed with $MKK5^{DD}$ in Arabidopsis protoplasts, and a slower mobility shift of BES1 was detected in the presence of $MKK5^{DD}$ (Fig. 4A), indicating that activation of MPK3/MPK6 by $MKK5^{DD}$ is sufficient to induce BES1 phosphorylation in the absence of PAMP perception. Previous study also showed that $MKK5^{K99M}$ inhibited BES1 phosphorylation induced by flg22 (Fig. 3D); hence, we concluded that BES1 phosphorylation triggered by PAMP occurs downstream of MKK4/MKK5-MPK3/MPK6 branch. Subsequently, we examined BES1 phosphorylation induced by flg22 in *mpk3* and *mpk6* single mutants. A slight reduction of BES1 phosphorylation induced by flg22 in *mpk6* mutant was detected by both regular SDS-PAGE (Fig. 4B) and Phos-tag SDS-PAGE followed by immunoblot (Fig. 4C). In the signaling pathway regulating stomatal patterning, $MPK6^{AEF}$ is a dominant negative mutant form that overcomes the redundancy of MPK3. We then further checked the effect of $MPK6^{AEF}$ on PAMP-triggered BES1 phosphorylation. As shown in Figure 4D, expression of $MPK6^{AEF}$, but not of MPK6, inhibited BES1 phosphorylation induced by flg22. The above results indicated that BES1 phosphorylation induced by flg22 is likely to occur downstream of MPK3/MPK6 branch. The partial reduction of BES1 phosphorylation induced by flg22 in *mpk6* mutant could be attributed to a putative functional redundancy with MPK3 or other MPKs. Normal BES1 phosphorylation induced by flg22 in *mpk3* mutant indicated that MPK3 is not essential for BES1 phosphorylation triggered by PAMP (Supplemental Fig. S4C).

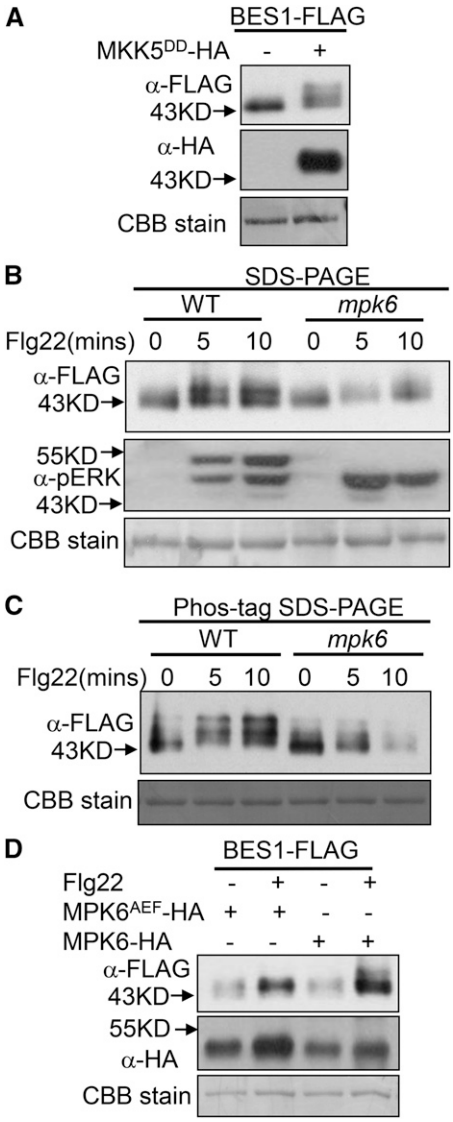

Figure 4. MPK6 activity is required for BES1 full phosphorylation induced by flg22. A, Coexpression of $MKK5^{DD}$ enhances BES1 phosphorylation. B and C, BES1 phosphorylation induced by flg22 is partially affected in *mpk6* mutant. D, Expression of $MPK6^{AEF}$ inhibits flg22-induced BES1 phosphorylation. Protoplasts isolated from wild-type (WT) or mutant plants were transfected with *35S::BES1-FLAG* or together with *35S::MKK5^{DD}-HA*, *35S::MPK6-HA*, or *35S::MPK6^{AEF}-HA* as indicated, treated with or without 1 μM flg22 for the indicated time. Protein samples were separated by SDS-PAGE (B) or Phos-tag SDS-PAGE (C) gel and subjected to anti-FLAG, anti-MPK6, or anti-phosphorylated extracellular signal-regulated kinase (pERK) immunoblot. Coomassie Brilliant Blue (CBB) staining of the filter indicates loading of the protein.

BES1 Is a Direct Substrate of MPK6

The above results raised the possibility of a physical protein-protein interaction between BES1 and MPK6. Purified glutathione *S*-transferase (GST), GST-tagged MPK6, MPK3, or MPK4 were incubated with an equal amount of purified His-BES1 and subjected to in vitro pull-down assay. GST-MPK6, but not GST-MPK3/MPK4 or GST, was detected to copurify with His-BES1 (Fig. 5A), indicating a direct and specific interaction between BES1 and MPK6 in vitro. The quantitative luciferase (LUC) complementation imaging assay was carried out to verify the specific interaction between BES1 and MPK6 in *Nicotiana benthamiana*. Coexpression of N-terminal of luciferase (NLuc)-tagged BIK1 and C-terminal of luciferase

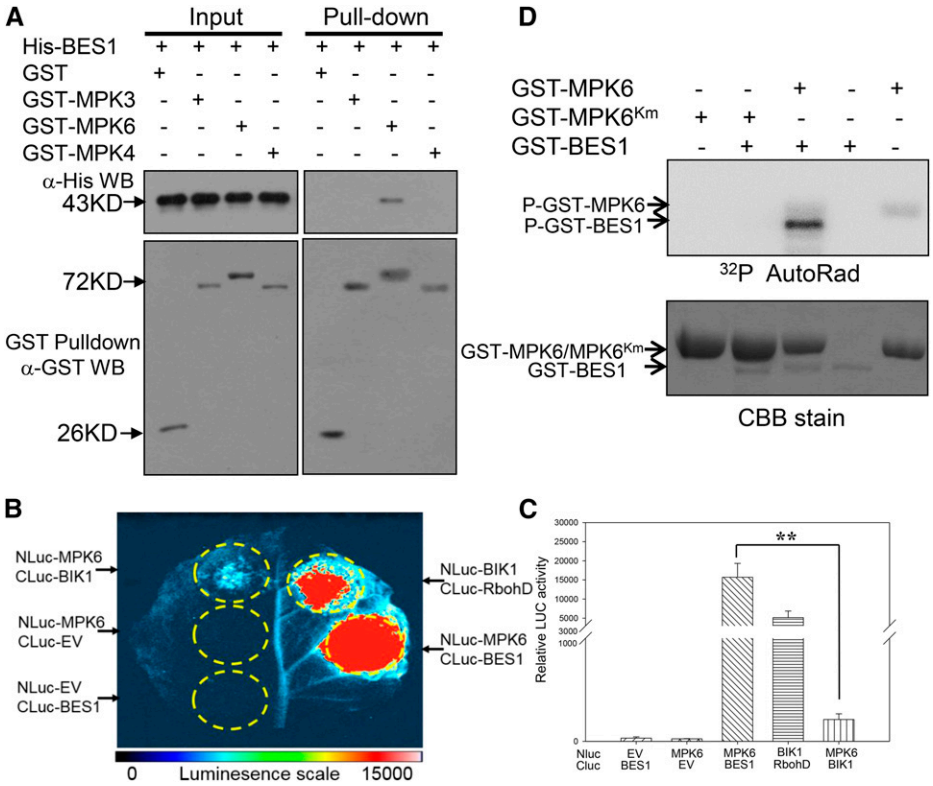

Figure 5. MPK6 interacts with and phosphorylates BES1. A, GST-MPK6 interacts with His-BES1 in vitro. An equal amount of His-BES1 was incubated with GST, GST-MPK6, GST-MPK3, or GST-MPK4, precipitated with glutathione agarose, and western-blot (WB) analysis was used to detect the presence of His-BES1. The amount of GST or His-tagged protein was determined by anti-GST or anti-His immunoblot. The experiment was repeated three times with similar results. B, Luciferase imaging of MPK6 and BES1 interaction in *N. benthamiana*. *N. benthamiana* leaves infiltrated with *35S::NLuc-MPK6*, *35S::CLuc-BES1*, *35S::CLuc-BIK1*, *35S::CLuc-AtrbohD*, *35S::NLuc-BIK1*, *35S::NLuc*, *or 35S::CLuc empty vector* (*EV*) as indicated were subjected to luciferase complementation imaging assay. C, Quantitative luminescence of MPK6 and BES1 interaction in *N. benthamiana*. *N. benthamiana* leaves infiltrated with indicated constructs were sliced into strips, and relative luminescence was determined by a microplate luminometer. Error bars indicate SD of three technical repeats. Asterisks indicate significant difference at $P < 0.01$. Similar results were observed in three independent biological repeats. NLuc, N-terminal fragment of firefly luciferase; CLuc, C-terminal fragment of firefly luciferase. D, BES1 is phosphorylated by MPK6 in vitro. GST-BES1, GST-MPK6, or GST-MPK6^{Km} alone and GST-BES1 incubated with GST-MPK6 or GST-MPK6^{Km} are subjected to in vitro phosphorylation assay. Coomassie Brilliant Blue (CBB) staining indicates loading of the protein. GST-MPK6^{Km} stands for MPK6 K92R mutation.

(CLuc)-tagged AtrbohD driven by 35S promoter was used as control for a positive interaction (Li et al., 2014). Coexpression of NLuc-MPK6 and CLuc-BES1 driven by 35S promoter in *N. benthamiana* resulted in much higher luciferase activity compared with coexpression of NLuc-MPK6 and CLuc-BIK1, NLuc-MPK6 and CLuc vector, or CLuc-BIK1 and NLuc vector (Fig. 5, B and C), indicating a specific interaction between BES1 and MPK6 in vivo. Expression levels of NLuc- and CLuc-fusion proteins were detected by immune blot (Supplemental Fig. S5). Thus, it was shown that MPK6 is able to interact with BES1 both in vitro and in vivo.

We then speculated a direct phosphorylation of BES1 by MPK6. In vitro phosphorylation assay was conducted to test whether BES1 was a direct substrate of MPK6. Purified His-BES1 or GST-BES1 alone did not exhibit autophosphorylation activity, whereas addition of purified GST-MPK6 resulted in phosphorylation of both His-BES1 and GST-BES1 in vitro (Supplemental Fig. S6). Meanwhile, GST-MPK6^{Km}, a kinase inactive mutant of MPK6, failed to phosphorylate BES1 in vitro (Fig. 5D). Thus, we concluded that BES1 is a direct substrate of MPK6 in vitro.

It is known that phosphorylation of BES1 by GSK3-like kinase BIN2 induce its nuclear export in BR signaling (Yin et al., 2002; Ryu et al., 2010). We next studied the effect of MAPK-mediated BES1 phosphorylation on its subcellular accumulation (Supplemental Materials and Methods S2). Expression of MKK5^{DD}, which phosphorylates MPK6 to constitutively activate PTI (Asai et al., 2002) and enhances BES1 phosphorylation, reduced the relative nucleus to cytoplasm ratio of BES1-GFP (Supplemental Fig. S7, A and B). The results suggested that MAPK-mediated phosphorylation alters BES1 subcellular accumulation in PTI.

BES1 S286 and S137 Residues Are Required for Full Phosphorylation Induced by flg22 and Bacterial Resistance

To determine BES1 phosphorylation sites targeted by activated MPK6, His-BES1 was incubated with MPK6 activated by $MKK5^{DD}$ (Asai et al., 2002). Phosphorylated BES1 was fractionated by SDS-PAGE and subjected to mass spectrometry analysis (Supplemental Materials and Methods S3). Several putative phosphorylation sites targeted by MPK6 were identified in BES1 (Supplemental Fig. S8). Because MAPKs are Pro-directed kinases (Kyriakis and Avruch, 2001), Ser residues that are immediately followed by Pro residue were selected as putative phosphorylation sites. Site-directed mutagenesis followed by mobility shift assay was conducted to identify critical sites required for BES1 phosphorylation induced by flg22. Of the potential residues identified by mass spectrometric analysis, $BES1^{S286A}$ mutation significantly impaired flg22-induced BES1 phosphorylation when $BES1^{S286A}$-FLAG was transiently expressed in protoplasts (Fig. 6A). Double mutation of BES1 S286A and S137A residues ($BES1^{SSAA}$) almost completely blocked BES1 phosphorylation induced by flg22 (Fig. 6A). We next studied in vivo phosphorylation of BES1 wild type and $BES1^{SSAA}$ protein in *BES1*::*BES1-FLAG* and *BES1*::$BES1^{SSAA}$*-FLAG* transgenic plants, respectively. In contrast to normal BES1 phosphorylation induced by flg22 in *BES1*::*BES1-FLAG* transgenic plants pretreated with or without epiBL, a significantly compromised $BES1^{SSAA}$ phosphorylation induced by flg22 was detected in *BES1*::$BES1^{SSAA}$*-FLAG* transgenic plants (Fig. 6B). The results indicated that S286 and S137 residues are required for flg22-induced BES1 full phosphorylation in vivo, in which S286 plays a greater role than S137.

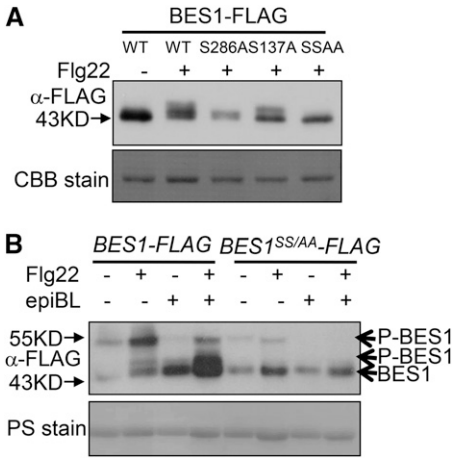

Figure 6. BES1 S286 and S137 are required for flg22-induced full phosphorylation. A, S286 and S137 are required for BES1 full phosphorylation induced by flg22 in protoplasts. Protoplasts were transfected with *35S*::*BES1-FLAG*, *35S*::$BES1^{S286A}$*-FLAG*, *35S*::$BES1^{S137A}$*-FLAG*, or *35S*::$BES1^{SSAA}$*-FLAG* as indicated, treated with or without flg22. B, S286 and S137 are required for BES1 full phosphorylation induced by flg22 in transgenic plants. *BES1*::*BES1-FLAG* or *BES1*::$BES1^{SSAA}$*-FLAG* transgenic plants were pretreated with or without 1 μM epiBL as indicated for 1 h, followed by 1 μM flg22 treatment. Protein samples were subjected to anti-FLAG immunoblot. Coomassie Brilliant Blue (CBB) or Ponceau S (PS) staining of the filter indicates loading of the protein. WT, Wild type.

$BES1^{SSAA}$ Impairs Plant Bacterial Resistance But Not BR-Mediated Hypocotyl and Root Growth

To determine the contribution of PAMP-induced BES1 phosphorylation in plant resistance, *bes1-1/BES1*::*BES1-FLAG* and *bes1-1/BES1*::$BES1^{SSAA}$*-FLAG* plants were constructed (Supplemental Fig. S9) and in planta bacterial growth of *Pst* DC3000 was examined in these transgenic lines (Fig. 7A). Hypocotyl length of *bes1-1* mutants was shorter than that of wild-type plants in response to brassinolide (BL) treatment (He et al., 2005), while hypocotyl length was comparable in *bes1-1/BES1*::*BES1-FLAG* plants and wild-type plants in response to BL (Fig. 7B), indicating that BES1::BES1-FLAG protein was functional. *BES1*::*BES1-FLAG*, but not *BES1*::$BES1^{SSAA}$*-FLAG*, could restore bacterial resistance of *bes1-1* mutant against *Pst* DC3000 (Fig. 7A), indicating that BES1 S286 and S137 are critical residues required both for phosphorylation triggered by PAMP and for full resistance against bacterial pathogen. Expression of BES1::BES1-FLAG and BES1::$BES1^{SSAA}$-FLAG in transgenic lines was confirmed by immune blot (Supplemental Fig. S10). As BR triggers dephosphorylation of BES1, an altered BR response in *bes1-1* mutant complemented with $BES1^{SSAA}$ would be expected if BES1 S286 and S137 residues are also required for BR signaling. To check the effect of $BES1^{SSAA}$ mutation on BR-mediated plant growth, hypocotyl and root length of *bes1-1* mutant complemented with BES1 wild type or $BES1^{SSAA}$ both in the absence or presence of epiBL was further examined. In contrast to a compromised bacterial resistance in *bes1-1/BES1*::$BES1^{SSAA}$*-FLAG* plants, a normal hypocotyl and root length was detected in *bes1-1/BES1*::$BES1^{SSAA}$*-FLAG* plants compared with *bes1-1/BES1*::*BES1-FLAG* plants, both in the absence or presence of epiBL (Fig. 7, B and C). We further examined the expression of BR-responsive genes in *bes1-1* mutant, *bes1-1/BES1*::*BES1-FLAG*, and *bes1-1/BES1*::$BES1^{SSAA}$*-FLAG* plants (Supplemental Materials and Methods S4). A compromised induction of *PACLOBUTRAZOL RESISTANCE1* (*PRE1*) and *PRE5* by epiBL was observed in *bes1-1* mutant (Supplemental Fig. S11, A and B). Both *BES1-FLAG* and $BES1^{SSAA}$*-FLAG* could restore *PRE1* and *PRE5* induction by epiBL in *bes1-1* mutant (Supplemental Fig. S11). The results indicated that BES1 S286 and S137 residues are not essential for BR-mediated plant growth. This is in agreement with previous reports that BES1 S129, S133, S171, and T175 are critical residues required for BR signaling (Ryu et al., 2007, 2010). Although the molecular mechanism by which BES1 phosphorylation regulates downstream PTI responses remains to be further clarified, different residue requirements of BES1 in PTI and BR signaling suggest differential modulation of a common transcription factor by plant hormone and immune signals. Additionally, the assumption that HDMs are recruited by BES1 to control defense-related gene expression is of interest for further investigation.

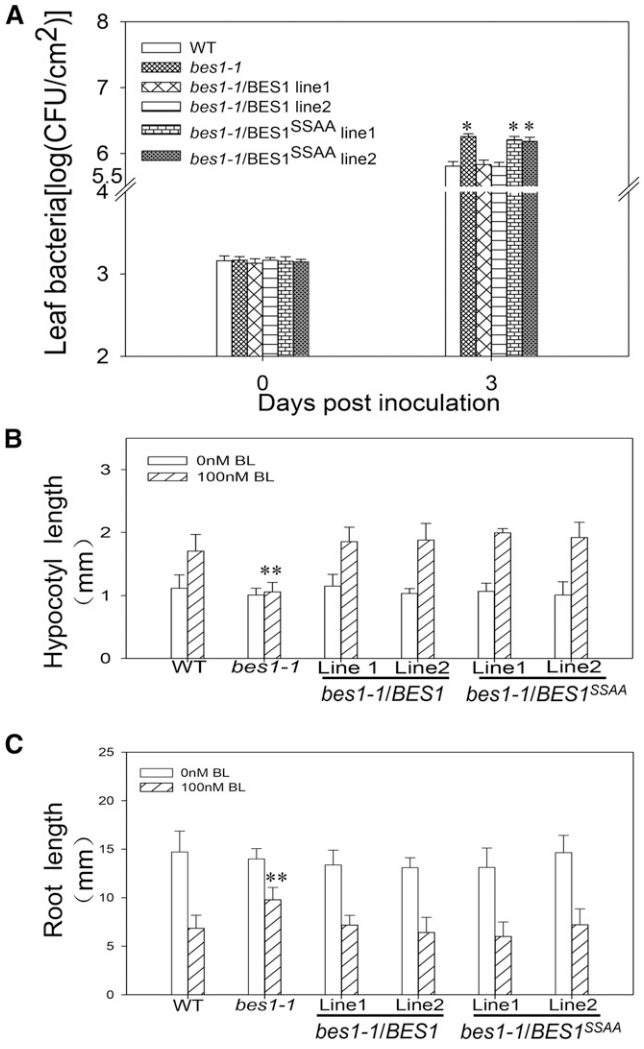

Figure 7. BES1^{SSAA} impairs bacterial resistance to *Pst* DC3000 but not BR-mediated hypocotyl and root growth. A, S286 and S137 are required for full resistance to *Pst* DC3000. Growth of *Pst* DC3000 in wild-type (WT), *bes1-1*, *bes1-1* complemented with BES1, or BES1^{SSAA} lines. The results shown are representative of three independent biological repeats. Error bars indicate SD of four technical repeats. Asterisk indicates significant difference to wild-type plants at $P < 0.05$. B and C, S286 and S137 are not required for BR-mediated hypocotyl (B) and root (C) growth. Hypocotyl and root lengths of long-day-grown wild-type, *bes1-1*, *bes1-1* complemented with BES1, or BES1^{SSAA} seedlings on medium containing 0 or 100 nM epiBL. Data are means ± SE ($n \geq 12$). Asterisks indicate significant difference to the 100 nM BL-treated wild type at $P < 0.01$. Similar results were observed in three independent biological repeats. GFP fluorescent *BES1*::*BES1-FLAG* and *BES1*::*BES1^{SSAA}-FLAG* T3 transgenic seeds were used for bacterial growth assay and hypocotyl and root growth assay.

DISCUSSION

PAMP recognition by PRR complex activates signaling kinases, such as MAPKs, calcium-dependent protein kinases, and BIK1/PBLs, to regulate downstream defense responses. However, only a few direct substrates of MAPKs in plant immune signaling have been identified, such as MKS1, AtPHOS32, AtERF104, VIP1, ACS2, and ACS6 (Peck et al., 2001; Liu and Zhang, 2004; Andreasson et al., 2005; Djamei et al., 2007; Merkouropoulos et al., 2008; Bethke et al., 2009; Han et al., 2010; Li et al., 2012). In addition, AtERF5 and AtERF6 transcription factors have also been reported as direct substrates of MPK6 and/or MPK3 that regulate plant immunity against fungal and bacterial pathogens, whereas their function in PTI is uncertain (Moffat et al., 2012; Son et al., 2012; Meng et al., 2013). Proteomic and phosphoproteomic approaches have been used to identify putative substrates for MAPKs in vivo; however, their biological significance requires further investigation (Peck et al., 2001; Merkouropoulos et al., 2008; Hoehenwarter et al., 2013). In this study, we show that BES1 is a direct substrate of MPK6 in PTI. In contrast to a reduced phosphorylation of BES1 in response to the plant hormone BR (Wang et al., 2002; Yin et al., 2005), an elevated BES1 phosphorylation upon bacterial PAMP perception was observed. PAMP perception triggers both the activation of MAPK cascades and the phosphorylation of BIK1/PBL1. We have previously shown that BIK1 and PBL1 are not required for MAPK activation in response to flg22 treatment (Feng et al., 2012), suggesting that BIK1/PBL1 phosphorylation and MAPK activation act in two branches. We found that PAMP-triggered BES1 phosphorylation is independent of BIK1 and PBL1, but it is suppressed when MAPK activity is inhibited. Hence, the results suggested a MAPK-dependent BES1 phosphorylation triggered by PAMP perception. Protein-protein interaction and protein phosphorylation studies demonstrate that BES1 associates with MPK6 and is phosphorylated by MPK6 upon PAMP perception. In addition, a comparison of BES1-direct target genes (Yu et al., 2011) with flg22-regulated genes showed that 234 out of 3,286 (7.1%) flg22-regulated genes (Chen et al., 2009) are BES1-direct target genes (14.5% of 1,609; Supplemental Fig. 12), indicating an important role of BES1 in PTI signaling.

We observed an elevated BES1 phosphorylation induced by flg22 both in Arabidopsis protoplasts and in 5-week-old mature transgenic plants grown under short-day conditions and treated with flg22 for 5 min. In a previous study, flg22 had been shown not to affect BES1 phosphorylation in 2-week-old transgenic seedlings treated with flg22 for 1.5 h (Albrecht et al., 2012). In addition to different plant growth conditions, the phosphorylation status of BES1 is also regulated by BR levels in plants and is affected by various environmental signals. Given that BR levels vary in plants throughout developmental stages, the phosphorylation status of BES1 may also vary. The conflicting results and different protein expression patterns in plants and protoplasts could be attributed to the differential BR levels due to developmental and environmental signals. Both in Arabidopsis protoplasts and in transgenic plants, Flg22 induced BES1 phosphorylation but not BES1^{SSAA} phosphorylation (Fig. 6, A and B). The flg22-induced BES1 phosphorylation could be partially masked by basal level of phosphorylated BES1, which was accumulated in untreated plants. Even though BES1 was almost completely dephosphorylated by epiBL pretreatment, the following flg22 treatment clearly resumed

BES1 phosphorylation in *BES1*::*BES1-FLAG* plants (Fig. 2B). These results demonstrate that PAMP induces BES1 phosphorylation at S286 and S137 residues in vivo and that the absence of flg22 effect on $BES1^{SSAA}$ phosphorylation is not a consequence of BR signaling preactivation.

Synergistic and antagonistic actions in plants constitute complex signal transduction networks between host immunity and hormone signaling that play an important role in balancing development with resistance. Recent studies revealed a complicated interplay between FLS2-mediated PTI signaling and BRI-mediated BR signaling pathways, which share a common coreceptor, BAK1 (Li et al., 2002; Wang and Chory, 2006; Chinchilla et al., 2007; Heese et al., 2007; Wang et al., 2008; Fan et al., 2014; Malinovsky et al., 2014). Both excess and reduced BR biosynthesis significantly compromised flg22-induced responses (Belkhadir et al., 2012). In addition to antagonistic and synergistic effect conferred by BAK1 competition, BR was also shown to inhibit PTI signaling either downstream or independently of BAK1 and BIK1 (Albrecht et al., 2012; Belkhadir et al., 2012). Additionally, BR-signaling kinase1 was reported to interact with FLS2 and regulate a subset of PTI signaling (Tang et al., 2008; Shi et al., 2013), while BIK1 was shown to negatively regulate BR signaling (Lin et al., 2013). BRASSINAZOLE RESISTANT1 cooperates with WRKY transcription factors and negatively regulates early PTI responses (Lozano-Durán et al., 2013). In this study, we demonstrate that MAPK-mediated BES1 phosphorylation induced by PAMP perception regulates plant immunity positively, which uncovers a different modulation of BES1 from the GSK3-like kinase BIN2-mediated BES1 phosphorylation in BR signaling (Yin et al., 2002, 2005; Ryu et al., 2010).

Perception of bacterial flagellin led to an elevation of BES1 phosphorylation. However, MAPK inactivation, via the expression of HopAI1, $MKK5^{K99M}$, or $MPK6^{AEF}$, inhibited PAMP-induced BES1 phosphorylation. The results indicate that PAMP perception enhances the phosphorylation of BES1 through pathogen-induced MAPKs. *bes1* mutant was compromised in resistance to bacterial pathogen and showed shorter hypocotyl length than wild-type plants in response to BL treatment (He et al., 2005). $BES1^{SSAA}$ restored BR-mediated plant growth but failed to restore the compromised resistance in *bes1* mutant (Fig. 7; Supplemental Figure S11), indicating that BES1 phosphorylation positively regulates plant immunity and that BES1 S286 and S137 phosphorylation was required for PTI but not for BR signaling. On the other hand, BES1 S129, S133, S171, and T175 have been identified as critical residues required for BR signaling (Ryu et al., 2007, 2010). These results indicate that differential modulation of BES1 phosphorylation is achieved by distinct upstream kinases in PTI and BR signaling. BES1 has also been demonstrated to be a substrate of more axillary growth locus2 (MAX2), a subunit of the S phase kinase-associated protein1-cullin-F box type ubiquitin E3 ligase, which regulates SL-responsive gene expression (Wang et al., 2013). The degradation rate of phosphorylated and dephosphorylated BES1 by MAX2 is different (Wang et al., 2013), suggesting a putative effect of BES1 phosphorylation status on SL signaling. Whether $BES1^{SSAA}$ mutation affects shoot branching is of interest for further investigation. Overall, these results indicate diverse modulation of BES1 targeted by distinct signaling proteins and a broad role of a common transcription factor in multiple hormones and immunity signaling pathways.

MATERIALS AND METHODS

Plants, Constructs, and Antibodies

Arabidopsis (*Arabidopsis thaliana*) plants used in this study include the Col-0 wild type and the *bes1-1* (He et al., 2005), *bes1-2* (Supplemental Fig. S1A), *bik1/pbl1* (Zhang et al., 2010), *summ2*, *mpk4/summ2*, *mkk1/mkk2/summ2* (Zhang et al., 2012), *mpk3*, and *mpk6-2* (Zhang et al., 2007) mutants. Constructs used in this study include $MKK5^{DD}$-His (Zhang et al., 2007), 35S-$BIK1^{K105E}$-HA (Zhang et al., 2010), and 35S-AtrbohD-Cluc (Li et al., 2014). pUC-FLAG (Li et al., 2005), pUC-Nluc, pUC-Cluc, pCambia1300-Nluc, and pCambia1300-Cluc (Chen et al., 2008) plasmid vectors were used to generate transient expression or transgenic expression constructs. The pFAST-G01 vector (Shimada et al., 2010) harboring a fluorescent OLEOSIN1-GFP marker that is specifically expressed on seed oil body membrane was used for *BES1*::*BES1-FLAG* and *BES1*::$BES1^{SSAA}$-*FLAG* transgenic plant construction, providing an immediate and nondestructive way of identifying transformed seeds under fluorescence microscopy. Other plants, constructs, and antibodies used were described in supporting information.

Bacterial Growth Assay

Five-week-old plants grown under short-day conditions were infiltrated with 10^5 cfu mL^{-1} *Pst* DC3000. Leaf bacterial number was determined at indicated days post inoculation. Each data point consisted of at least three replicates. GFP fluorescent *BES1*::*BES1-FLAG* and *BES1*::$BES1^{SSAA}$-*FLAG* T3 transgenic seeds were used for bacterial growth assay, and the expression of BES1::BES1-FLAG and BES1::$BES1^{SSAA}$-FLAG protein was further confirmed by immune blot.

Quantitative Reverse Transcription-PCR

Five-week-old plants were treated with or without 500 nM flg22 or 100 nM epiBL as indicated for 3 h. Total RNA was extracted with TRIZOL (Invitrogen) and used for reverse transcription. Real-Time PCR was performed by using SYBR Premix Ex Taq kit (TaKaRa) following standard protocols. The housekeeping gene *TUBLIN* was used as internal control.

Transient Expression in Protoplast

Protoplasts isolated from 5-week-old plants were transfected with the indicated constructs. Twelve hours after transfection, protoplasts were treated with 1 μM flg22 or water as indicated for 5 min.

Detection of BES1 Phosphorylation in Protoplast and Plant

Protoplasts transfected with constructs as indicated were treated with 1 μM flg22 or water. Five-week-old *BES1*::*BES1-FLAG* transgenic plants were infiltrated with 1 μM flg22 or water. One micromolar epiBL was infiltrated into plants 1 h before flg22 treatment in BL-pretreated experiments. For phosphatase treatment, total protein was treated with λ PPase (New England Biolabs) according to manufacturer's instruction. In Phos-tag SDS-PAGE assay, SDS-PAGE gel supplied with 20 μM Phos-tag was used for electrophoresis. Total protein was extracted and subjected to anti-FLAG immunoblot.

GST Pull-Down Assay

GST, GST-MPK6, GST-MPK3, GST-MPK4, or His-BES1 was expressed in *Escherichia coli* and purified. An equal amount of the purified His-BES1 was incubated with GST, GST-MPK6, GST-MPK3, or GST-MPK4 as indicated for 4 h and then passed through the glutathione agarose column. The column

was washed four times, and bound protein was boiled and separated by SDS-PAGE gel.

Luciferase Complementation Imaging Assay

Agrobacterium tumefaciens strains carrying CLuc and NLuc constructs were mixed and infiltrated into leaves of *Nicotiana benthamiana*. Leaves coexpressing different constructs were examined for LUC activity 2 d after infiltration. *N. benthamiana* leaves were kept in dark for 5 min after adding 1 mM luciferin to quench the fluorescence. LUC image was captured by cooled CCD imaging apparatus (Roper Scientific). Quantitative LUC activity was determined by Microplate Luminometer (Promega). Expression of CLuc-tagged proteins and NLuc-tagged proteins was detected by anti-CLuc or anti-Luc immunoblot.

Hypocotyl and Root Growth Assay

Arabidopsis Col-0 wild-type, *bes1-1* mutant, and GFP fluorescent *BES1*::*BES1-FLAG* and *BES1*::*BES1*^{SSAA}*-FLAG* T3 transgenic seeds were surface sterilized and plated on one-half-strength Murashige and Skoog medium supplemented with 9 g L^{-1} agar and 10 g L^{-1} Suc with or without epiBL as indicated. Seedlings were grown under long-day conditions for 6 d after 2 d of incubation at 4°C, and hypocotyl and root length was measured.

Supplemental Data

The following supplemental materials are available.

Supplemental Figure S1. Characterization and disease symptom of *bes1-1* and *bes1-2* mutants.

Supplemental Figure S2. Chitin and Elf18 induce BES1 phosphorylation.

Supplemental Figure S3. Normal flg22-induced MAPK activation in *bes1-1* and *bes1-2* mutants.

Supplemental Figure S4. Mutation of *MPK4*, *MKK1/MKK2*, or *MPK3* is not sufficient to block flg22-induced BES1 phosphorylation.

Supplemental Figure S5. Expression levels of NLuc- and CLuc-fusion proteins in *N. benthamiana*.

Supplemental Figure S6. BES1 is phosphorylated by MPK6 in vitro.

Supplemental Figure S7. Coexpression of MKK5DD reduced nucleus accumulation of BES1-GFP in Arabidopsis protoplasts.

Supplemental Figure S8. Mass spectrometry analysis of BES1 phosphorylation sites.

Supplemental Figure S9. Morphologic phenotype of *bes1-1*, *bes1-1/BES1*::*BES1-FLAG*, and *bes1-1/BES1*::*BES1*^{SSAA}*-FLAG* plants.

Supplemental Figure S10. Expression levels of BES1-FLAG and BES1^{SSAA}-FLAG in *bes1-1/BES1*::*BES1-FLAG* and *bes1-1/BES1*::*BES1*^{SSAA}*-FLAG* plants.

Supplemental Figure S11. BES1 S286 and S137 are not required for the induction of *PRE1* and *PRE5* by epiBL.

Supplemental Figure S12. A comparison of BES1-direct target genes with flg22-regulated genes.

Supplemental Materials and Methods S1. Plants, constructs, and antibodies.

Supplemental Materials and Methods S2. Fluorescence microscopy.

Supplemental Materials and Methods S3. Mass spectrometric analysis.

Supplemental Materials and Methods S4. Primers used in the study.

ACKNOWLEDGMENTS

We thank Jian-min Zhou (Institute of Genetics and Developmental Biology, Chinese Academy of Sciences) for sharing biological materials and providing reagents, Yuelin Zhang (University of British Columbia) for *summ2*, *mpk4/summ2*, and *mkk1/mkk2/summ2* seeds, and Daoxin Xie (Tsinghua University) for *bes1-1* seeds.

Received September 24, 2014; accepted January 20, 2015; published January 21, 2015.

LITERATURE CITED

Albrecht C, Boutrot F, Segonzac C, Schwessinger B, Gimenez-Ibanez S, Chinchilla D, Rathjen JP, de Vries SC, Zipfel C (2012) Brassinosteroids inhibit pathogen-associated molecular pattern-triggered immune signaling independent of the receptor kinase BAK1. Proc Natl Acad Sci USA **109:** 303–308

Alvarez-Venegas R, Abdallat AA, Guo M, Alfano JR, Avramova Z (2007) Epigenetic control of a transcription factor at the cross section of two antagonistic pathways. Epigenetics **2:** 106–113

Andreasson E, Jenkins T, Brodersen P, Thorgrimsen S, Petersen NH, Zhu S, Qiu JL, Micheelsen P, Rocher A, Petersen M, et al (2005) The MAP kinase substrate MKS1 is a regulator of plant defense responses. EMBO J **24:** 2579–2589

Asai T, Tena G, Plotnikova J, Willmann MR, Chiu WL, Gomez-Gomez L, Boller T, Ausubel FM, Sheen J (2002) MAP kinase signalling cascade in Arabidopsis innate immunity. Nature **415:** 977–983

Belkhadir Y, Jaillais Y, Epple P, Balsemão-Pires E, Dangl JL, Chory J (2012) Brassinosteroids modulate the efficiency of plant immune responses to microbe-associated molecular patterns. Proc Natl Acad Sci USA **109:** 297–302

Berr A, McCallum EJ, Alioua A, Heintz D, Heitz T, Shen WH (2010) Arabidopsis histone methyltransferase SET DOMAIN GROUP8 mediates induction of the jasmonate/ethylene pathway genes in plant defense response to necrotrophic fungi. Plant Physiol **154:** 1403–1414

Bethke G, Unthan T, Uhrig JF, Pöschl Y, Gust AA, Scheel D, Lee J (2009) Flg22 regulates the release of an ethylene response factor substrate from MAP kinase 6 in *Arabidopsis thaliana* via ethylene signaling. Proc Natl Acad Sci USA **106:** 8067–8072

Boudsocq M, Willmann MR, McCormack M, Lee H, Shan L, He P, Bush J, Cheng SH, Sheen J (2010) Differential innate immune signalling via Ca^{2+} sensor protein kinases. Nature **464:** 418–422

Chen H, Xue L, Chintamanani S, Germain H, Lin H, Cui H, Cai R, Zuo J, Tang X, Li X, et al (2009) ETHYLENE INSENSITIVE3 and ETHYLENE INSENSITIVE3-LIKE1 repress *SALICYLIC ACID INDUCTION DEFICIENT2* expression to negatively regulate plant innate immunity in *Arabidopsis*. Plant Cell **21:** 2527–2540

Chen H, Zou Y, Shang Y, Lin H, Wang Y, Cai R, Tang X, Zhou JM (2008) Firefly luciferase complementation imaging assay for protein-protein interactions in plants. Plant Physiol **146:** 368–376

Chinchilla D, Bauer Z, Regenass M, Boller T, Felix G (2006) The *Arabidopsis* receptor kinase FLS2 binds flg22 and determines the specificity of flagellin perception. Plant Cell **18:** 465–476

Chinchilla D, Zipfel C, Robatzek S, Kemmerling B, Nürnberger T, Jones JD, Felix G, Boller T (2007) A flagellin-induced complex of the receptor FLS2 and BAK1 initiates plant defence. Nature **448:** 497–500

Djamei A, Pitzschke A, Nakagami H, Rajh I, Hirt H (2007) Trojan horse strategy in *Agrobacterium* transformation: abusing MAPK defense signaling. Science **318:** 453–456

Fan M, Bai MY, Kim JG, Wang T, Oh E, Chen L, Park CH, Son SH, Kim SK, Mudgett MB, et al (2014) The bHLH transcription factor HBI1 mediates the trade-off between growth and pathogen-associated molecular pattern-triggered immunity in *Arabidopsis*. Plant Cell **26:** 828–841

Feng F, Yang F, Rong W, Wu X, Zhang J, Chen S, He C, Zhou JM (2012) A *Xanthomonas* uridine 5′-monophosphate transferase inhibits plant immune kinases. Nature **485:** 114–118

Gómez-Gómez L, Boller T (2000) FLS2: an LRR receptor-like kinase involved in the perception of the bacterial elicitor flagellin in Arabidopsis. Mol Cell **5:** 1003–1011

Gómez-Gómez L, Felix G, Boller T (1999) A single locus determines sensitivity to bacterial flagellin in *Arabidopsis thaliana*. Plant J **18:** 277–284

Han L, Li GJ, Yang KY, Mao G, Wang R, Liu Y, Zhang S (2010) Mitogen-activated protein kinase 3 and 6 regulate *Botrytis cinerea*-induced ethylene production in Arabidopsis. Plant J **64:** 114–127

He JX, Gendron JM, Sun Y, Gampala SS, Gendron N, Sun CQ, Wang ZY (2005) BZR1 is a transcriptional repressor with dual roles in brassinosteroid homeostasis and growth responses. Science **307:** 1634–1638

Heese A, Hann DR, Gimenez-Ibanez S, Jones AM, He K, Li J, Schroeder JI, Peck SC, Rathjen JP (2007) The receptor-like kinase SERK3/BAK1 is a central regulator of innate immunity in plants. Proc Natl Acad Sci USA **104:** 12217–12222

Hoehenwarter W, Thomas M, Nukarinen E, Egelhofer V, Röhrig H, Weckwerth W, Conrath U, Beckers GJ (2013) Identification of novel in

vivo MAP kinase substrates in *Arabidopsis thaliana* through use of tandem metal oxide affinity chromatography. Mol Cell Proteomics **12:** 369–380

Kadota Y, Sklenar J, Derbyshire P, Stransfeld L, Asai S, Ntoukakis V, Jones JD, Shirasu K, Menke F, Jones A, et al (2014) Direct regulation of the NADPH oxidase RBOHD by the PRR-associated kinase BIK1 during plant immunity. Mol Cell **54:** 43–55

Kyriakis JM, Avruch J (2001) Mammalian mitogen-activated protein kinase signal transduction pathways activated by stress and inflammation. Physiol Rev **81:** 807–869

Li G, Meng X, Wang R, Mao G, Han L, Liu Y, Zhang S (2012) Dual-level regulation of ACC synthase activity by MPK3/MPK6 cascade and its downstream WRKY transcription factor during ethylene induction in Arabidopsis. PLoS Genet **8:** e1002767

Li J, Wen J, Lease KA, Doke JT, Tax FE, Walker JC (2002) BAK1, an Arabidopsis LRR receptor-like protein kinase, interacts with BRI1 and modulates brassinosteroid signaling. Cell **110:** 213–222

Li L, Li M, Yu L, Zhou Z, Liang X, Liu Z, Cai G, Gao L, Zhang X, Wang Y, et al (2014) The FLS2-associated kinase BIK1 directly phosphorylates the NADPH oxidase RbohD to control plant immunity. Cell Host Microbe **15:** 329–338

Li X, Lin H, Zhang W, Zou Y, Zhang J, Tang X, Zhou JM (2005) Flagellin induces innate immunity in nonhost interactions that is suppressed by *Pseudomonas syringae* effectors. Proc Natl Acad Sci USA **102:** 12990–12995

Lin W, Lu D, Gao X, Jiang S, Ma X, Wang Z, Mengiste T, He P, Shan L (2013) Inverse modulation of plant immune and brassinosteroid signaling pathways by the receptor-like cytoplasmic kinase BIK1. Proc Natl Acad Sci USA **110:** 12114–12119

Liu Y, Zhang S (2004) Phosphorylation of 1-aminocyclopropane-1-carboxylic acid synthase by MPK6, a stress-responsive mitogen-activated protein kinase, induces ethylene biosynthesis in *Arabidopsis*. Plant Cell **16:** 3386–3399

Lozano-Durán R, Macho AP, Boutrot F, Segonzac C, Somssich IE, Zipfel C (2013) The transcriptional regulator BZR1 mediates trade-off between plant innate immunity and growth. eLife **2:** e00983

Lu D, Lin W, Gao X, Wu S, Cheng C, Avila J, Heese A, Devarenne TP, He P, Shan L (2011) Direct ubiquitination of pattern recognition receptor FLS2 attenuates plant innate immunity. Science **332:** 1439–1442

Lu D, Wu S, Gao X, Zhang Y, Shan L, He P (2010) A receptor-like cytoplasmic kinase, BIK1, associates with a flagellin receptor complex to initiate plant innate immunity. Proc Natl Acad Sci USA **107:** 496–501

Malinovsky FG, Batoux M, Schwessinger B, Youn JH, Stransfeld L, Win J, Kim SK, Zipfel C (2014) Antagonistic regulation of growth and immunity by the Arabidopsis basic helix-loop-helix transcription factor HOMOLOG OF BRASSINOSTEROID ENHANCED EXPRESSION2 INTERACTING WITH INCREASED LEAF INCLINATION1 BINDING bHLH1. Plant Physiol **164:** 1443–1455

Meng X, Xu J, He Y, Yang KY, Mordorski B, Liu Y, Zhang S (2013) Phosphorylation of an ERF transcription factor by *Arabidopsis* MPK3/MPK6 regulates plant defense gene induction and fungal resistance. Plant Cell **25:** 1126–1142

Merkouropoulos G, Andreasson E, Hess D, Boller T, Peck SC (2008) An Arabidopsis protein phosphorylated in response to microbial elicitation, AtPHOS32, is a substrate of MAP kinases 3 and 6. J Biol Chem **283:** 10493–10499

Moffat CS, Ingle RA, Wathugala DL, Saunders NJ, Knight H, Knight MR (2012) ERF5 and ERF6 play redundant roles as positive regulators of JA/Et-mediated defense against *Botrytis cinerea* in Arabidopsis. PLoS ONE **7:** e35995

Peck SC, Nühse TS, Hess D, Iglesias A, Meins F, Boller T (2001) Directed proteomics identifies a plant-specific protein rapidly phosphorylated in response to bacterial and fungal elicitors. Plant Cell **13:** 1467–1475

Petersen M, Brodersen P, Naested H, Andreasson E, Lindhart U, Johansen B, Nielsen HB, Lacy M, Austin MJ, Parker JE, et al (2000) Arabidopsis map kinase 4 negatively regulates systemic acquired resistance. Cell **103:** 1111–1120

Pitzschke A, Schikora A, Hirt H (2009) MAPK cascade signalling networks in plant defence. Curr Opin Plant Biol **12:** 421–426

Ryu H, Cho H, Kim K, Hwang I (2010) Phosphorylation dependent nucleocytoplasmic shuttling of BES1 is a key regulatory event in brassinosteroid signaling. Mol Cells **29:** 283–290

Ryu H, Kim K, Cho H, Park J, Choe S, Hwang I (2007) Nucleocytoplasmic shuttling of BZR1 mediated by phosphorylation is essential in *Arabidopsis* brassinosteroid signaling. Plant Cell **19:** 2749–2762

Schwessinger B, Zipfel C (2008) News from the frontline: recent insights into PAMP-triggered immunity in plants. Curr Opin Plant Biol **11:** 389–395

Shi H, Shen Q, Qi Y, Yan H, Nie H, Chen Y, Zhao T, Katagiri F, Tang D (2013) BR-SIGNALING KINASE1 physically associates with FLAGELLIN SENSING2 and regulates plant innate immunity in *Arabidopsis*. Plant Cell **25:** 1143–1157

Shimada TL, Shimada T, Hara-Nishimura I (2010) A rapid and non-destructive screenable marker, FAST, for identifying transformed seeds of *Arabidopsis thaliana*. Plant J **61:** 519–528

Son GH, Wan J, Kim HJ, Nguyen XC, Chung WS, Hong JC, Stacey G (2012) Ethylene-responsive element-binding factor 5, ERF5, is involved in chitin-induced innate immunity response. Mol Plant Microbe Interact **25:** 48–60

Sun Y, Li L, Macho AP, Han Z, Hu Z, Zipfel C, Zhou JM, Chai J (2013) Structural basis for flg22-induced activation of the Arabidopsis FLS2-BAK1 immune complex. Science **342:** 624–628

Tang W, Kim TW, Oses-Prieto JA, Sun Y, Deng Z, Zhu S, Wang R, Burlingame AL, Wang ZY (2008) BSKs mediate signal transduction from the receptor kinase BRI1 in Arabidopsis. Science **321:** 557–560

Veronese P, Nakagami H, Bluhm B, Abuqamar S, Chen X, Salmeron J, Dietrich RA, Hirt H, Mengiste T (2006) The membrane-anchored BOTRYTIS-INDUCED KINASE1 plays distinct roles in *Arabidopsis* resistance to necrotrophic and biotrophic pathogens. Plant Cell **18:** 257–273

Wang X, Chory J (2006) Brassinosteroids regulate dissociation of BKI1, a negative regulator of BRI1 signaling, from the plasma membrane. Science **313:** 1118–1122

Wang X, Kota U, He K, Blackburn K, Li J, Goshe MB, Huber SC, Clouse SD (2008) Sequential transphosphorylation of the BRI1/BAK1 receptor kinase complex impacts early events in brassinosteroid signaling. Dev Cell **15:** 220–235

Wang Y, Sun S, Zhu W, Jia K, Yang H, Wang X (2013) Strigolactone/MAX2-induced degradation of brassinosteroid transcriptional effector BES1 regulates shoot branching. Dev Cell **27:** 681–688

Wang ZY, Nakano T, Gendron J, He J, Chen M, Vafeados D, Yang Y, Fujioka S, Yoshida S, Asami T, et al (2002) Nuclear-localized BZR1 mediates brassinosteroid-induced growth and feedback suppression of brassinosteroid biosynthesis. Dev Cell **2:** 505–513

Yin Y, Vafeados D, Tao Y, Yoshida S, Asami T, Chory J (2005) A new class of transcription factors mediates brassinosteroid-regulated gene expression in Arabidopsis. Cell **120:** 249–259

Yin Y, Wang ZY, Mora-Garcia S, Li J, Yoshida S, Asami T, Chory J (2002) BES1 accumulates in the nucleus in response to brassinosteroids to regulate gene expression and promote stem elongation. Cell **109:** 181–191

Yu X, Li L, Li L, Guo M, Chory J, Yin Y (2008) Modulation of brassinosteroid-regulated gene expression by Jumonji domain-containing proteins ELF6 and REF6 in Arabidopsis. Proc Natl Acad Sci USA **105:** 7618–7623

Yu X, Li L, Zola J, Aluru M, Ye H, Foudree A, Guo H, Anderson S, Aluru S, Liu P, et al (2011) A brassinosteroid transcriptional network revealed by genome-wide identification of BESI target genes in *Arabidopsis thaliana*. Plant J **65:** 634–646

Zhang J, Li W, Xiang T, Liu Z, Laluk K, Ding X, Zou Y, Gao M, Zhang X, Chen S, et al (2010) Receptor-like cytoplasmic kinases integrate signaling from multiple plant immune receptors and are targeted by a *Pseudomonas syringae* effector. Cell Host Microbe **7:** 290–301

Zhang J, Shao F, Li Y, Cui H, Chen L, Li H, Zou Y, Long C, Lan L, Chai J, et al (2007) A *Pseudomonas syringae* effector inactivates MAPKs to suppress PAMP-induced immunity in plants. Cell Host Microbe **1:** 175–185

Zhang J, Zhou JM (2010) Plant immunity triggered by microbial molecular signatures. Mol Plant **3:** 783–793

Zhang Z, Wu Y, Gao M, Zhang J, Kong Q, Liu Y, Ba H, Zhou J, Zhang Y (2012) Disruption of PAMP-induced MAP kinase cascade by a *Pseudomonas syringae* effector activates plant immunity mediated by the NB-LRR protein SUMM2. Cell Host Microbe **11:** 253–263

Zipfel C, Kunze G, Chinchilla D, Caniard A, Jones JD, Boller T, Felix G (2006) Perception of the bacterial PAMP EF-Tu by the receptor EFR restricts *Agrobacterium*-mediated transformation. Cell **125:** 749–760

Supplemental Data

The Arabidopsis Transcription Factor BES1 Is a Direct Substrate of MPK6 and Regulates Immunity

Authors: Sining Kang, Fan Yang, Lin Li, Huamin Chen, She Chen and Jie Zhang

The following Supplemental Data is available for this article:

Supplemental Figures

Figure S1. Characterization and disease symptom of *bes1-1* and *bes1-2* mutants.

A, Schematic presentation of T-DNA insertions in *BES1*. Boxes denote predicated open reading frames. Inverted triangle indicates position of T-DNA insertion. B, Disease symptom of 5-week-old WT, *bes1-1* and *bes1-2* plant leaves. Leaves infiltrated with 10^6 CFU ml^{-1} *Pst* DC3000 were photographed 3 days post inoculation. C, Quantitative RT-PCR analysis of *BES1* transcript levels in *bes1-1* and *bes1-2* mutants. Total RNA of 5-week-old plants was extracted and used for reverse transcription. Real-Time PCR was performed following standard protocols. Values are normalized to *TUBLIN* control. Error bars indicate standard deviation of 3 technical repeats. ** indicates significant difference at *P* value <0.01. Similar results were observed in 3 independent biological repeats.

Figure S2. Chitin and Elf18 induce BES1 phosphorylation.

CSC (Crab shell chitin) and Elf18 (an *N*-acetylated peptide comprising the first 18 amino acids of EF-Tu) induce BES1 phosphorylation in protoplasts. Col-0 protoplasts were transfected with *35S::BES1-FLAG*, treated with 1 μM flg22, 200 mg ml^{-1} csc or 1 μM elf18 respectively for 5 minutes. Total proteins extracted from protoplasts were separated by SDS-PAGE and subjected to anti-FLAG immunoblot. Ponceau S (PS) staining of the filter indicates loading of the protein.

Figure S3. Normal flg22-induced MAPK activation in *bes1-1* and *bes1-2* mutants.

Flg22 induces comparable MAPK activation in *bes1-1*, *bes1-2* and WT plants. WT and mutant plants were sprayed with 10 μM flg22 or H_2O for the indicated time. Protein samples were separated by SDS-PAGE and subjected to anti-pERK immunoblot. CBB staining of the filter indicates loading of the protein.

Figure S4. Mutation of *MPK4*, *MKK1/2* or *MPK3* is not sufficient to block flg22-induced BES1 phosphorylation.

A, BES1 phosphorylation induced by flg22 in *mkk1/mkk2/summ2* mutant. **B**, BES1 phosphorylation induced by flg22 in *mpk4/summ2* mutant. Protoplasts isolated from WT, *summ2*, *mpk4/summ2* or *mkk1/mkk2/summ2* mutant were transfected with *35S::BES1-FLAG*, treated with or without flg22. C, BES1 phosphorylation induced by flg22 in *mpk3* mutant. Col-0 and *mpk3* mutant protoplasts were transfected with *35S::BES1-FLAG*, treated with or without 1 μM flg22. Protein samples were separated by SDS-PAGE and subjected to anti-FLAG immunoblot. PS or CBB staining of the filter indicates loading of the protein.

Figure S5. Expression levels of NLuc- and CLuc-fusion proteins in *Nicotiana benthamiana*.

A, NLuc-fusion proteins was detected by anti-Luc immune-blot. B, CLuc-fusion proteins was detected by anti-CLuc immune-blot. CBB staining of the filter indicates loading of the protein.

Figure S6. BES1 is phosphorylated by MPK6 *in vitro*.

GST-BES1 or His-BES1 was incubated with GST-MPK6 and subjected to *in vitro* phosphorylation assay. CBB staining indicates loading of the protein.

Figure S7. Co-expression of $MKK5^{DD}$ reduced nucleus accumulation of BES1-GFP in Arabidopsis protoplasts.

A, Representative confocal image of BES1-GFP subcellular accumulation. GFP-fluorescent cells were indicated by arrows. B, Quantitative relative nucleus to

cytoplasm ratio of BES1-GFP. Protoplasts were transfected with *35S::BES1-GFP* alone, or together with *35S::MKK5* or *35S::BIN2* as indicated. The subcellular locations of BES1-GFP were examined using Leica SP8 confocal microscopy 8 hours after transfection. The intensities of the nucleus and cytoplasm fluorescent signals of 30 cells in each treatment was determined by Leica LAS AF Lite software. Data are means ± SE (n = 30). ** indicates significant difference at *P* value <0.01. Similar results were observed in 3 independent biological repeats.

Figure S8. Mass spectrometry analysis of BES1 phosphorylation sites.

A, Peptide sequences containing potential phosphorylation sites phosphorylated by MPK6 activated by $MKK5^{DD}$. p indicates phosphorylation of the following residue. B, Mass spectrometry analysis of S286 residue. C, Mass spectrometry analysis of S137 and S129 residues.

Figure S9. Morphologic phenotype of *bes1-1, bes1-1*/*BES1::BES1-FLAG* and *bes1-1*/*BES1::BES1^{SSAA}-FLAG* plants.

5-week-old WT, *bes1-1*, *bes1-1*/*BES1::BES1-FLAG* and *bes1-1*/*BES1::BES1^{SSAA}-FLAG* plants grown under short-day conditions were photographed.

Figure S10. Expression levels of BES1-FLAG and $BES1^{SSAA}$-FLAG in *bes1-1*/ *BES1::BES1-FLAG* and *bes1-1*/ *BES1::BES1^{SSAA}-FLAG* plants.

Transgenic seeds carrying GFP fluorescence in seed oil body membrane were selected and then used for the experiments in this study. The expression levels of the transgenes was further confirmed by western blot. Total protein extracted from leaves was separated by SDS-PAGE and subjected to anti-FLAG immunoblot. CBB staining of the filter indicates loading of the protein. Results shown are representative of transgene expression in *bes1*/*BES1::BES1-FLAG* and *bes1*/*BES1::BES1^{SSAA}-FLAG* line 1 (A) and line 2 (B) transgenic lines.

Figure S11. BES1 S286 and S137 are not required for the induction of *PRE1* and

***PRE5* by epiBL.**

5-week-old WT, *bes1-1*, *bes1*/*BES1::BES1-FLAG* and *bes1*/*BES1::BES1*^{SSAA}*-FLAG* plants were treated with or without 100 nM epiBL for 3 hours. Expression of *PRE1* (A), *PRE5* (B), *BZR1* (C), *BR6OX2* and *CPD* (D) was measured by Real-Time PCR. Total RNA from leaves was extracted and used for reverse transcription. Real-Time PCR was performed following standard protocols. Values are normalized to *TUBLIN* control and are presented as relative to the value of 0nM epiBL-treated WT plants. Error bars indicate standard deviation of 3 technical repeats. ** indicates significant difference to 100nM epiBL-treated WT plants at *P* value <0.01. Similar results were observed in 3 independent biological repeats.

Figure S12. A comparison of BES1-direct target genes (Yu et al., 2011) with flg22-regulated genes (Chen et al., 2009).

Venn diagram shows overlaps among BES1-direct target genes and flg22-regulated genes.

Supplemental Materials and Methods

Materials and Methods S1 Plants, constructs and antibodies

BES1 genomic DNA containing the promoter and coding sequence was amplified from WT plants and cloned into pFAST-G01 to generate pFAST-*BES1::BES1-FLAG* plasmid. pFAST-*BES1::BES1-FLAG* was introduced into Col-0 and *bes1-1* to generate *BES1::BES1-FLAG* and *bes1-1/BES1* transgenic plants respectively. *BES1::BES1*^{SSAA}*-FLAG* construct were generated by site-directed mutagenesis, and introduced into Col-0 and *bes1-1* to generate *BES1::BES1*^{SSAA}*-FLAG* and *bes1-1/ BES1*^{SSAA} transgenic plants respectively. The *BES1* cDNA was amplified by RT-PCR from WT total RNA to generate the His-BES1, GST-BES1 and BES1-FLAG construct. The *MKK5* cDNA was amplified by RT-PCR from WT plants total RNA to generate MKK5-HA plasmid. The *MPK6*, *BES1*, *BIK1* cDNA was amplified by RT-PCR from WT total RNA to generate MPK6-Nluc, BES1-Cluc, BIK1-Cluc, BIK1-Nluc, Cluc-MPK6, BES1-Nluc plasmid. BES1^{S137A}, BES1^{S286A}, BES1^{SSAA} and MKK5^{K99M} mutant plasmids were generated by

site-directed mutagenesis. Other constructs used include HopAI1-FLAG, GST-MPK6, GST-MPK3 and $MKK5^{DD}$-HA. Antibodies used include anti-FLAG, anti-His monoclonal antibody and anti-MPK6 polyclonal antibody (Sigma-Aldrich), anti-HA monoclonal，anti-GST monoclonal antibody (TianGen, Beijing), anti-phospho-p44/42 MAPK (pERK) polyclonal antibody (Cell Signaling), anti-CLUC monoclonal antibody and anti-LUC polyclonalantibody (Sigma-Aldrich).

Materials and Methods S2 Fluorescence Microscopy

Protoplasts were transfected with *35S::BES1-GFP* alone, or together with *35S::MKK5^{DD}-HA* or *35S::BIN2-HA* as indicated. GFP fluorescence was observed with Leica SP8 confocal microscopy 8 hours after transfection. The intensities of the nucleus and cytoplasm fluorescent signals was determined by Leica LAS AF Lite software.

Materials and Methods S3 Mass spectrometric analysis

Recombinant BES1-His was incubated in 20 μl kinase reaction buffer with $MKK5^{DD}$-activated MPK6 for 30 minutes and electrophoresed through a SDS-PAGE. Protein bands were de-stained, and then reduced in 10 mM DTT at 56 °C for 30 min followed by alkylation in 55 mM iodoacetamide. After washing with ultra-pure water twice, the gel bands were dehydrated by acetonitrile, and then digested in gel with sequencing grade trypsin (10 ng μl^{-1} trypsin, 50 mM ammonium bicarbonate, pH 8.0) overnight at 37 ℃. Peptides were extracted with 5% formic acid/50% acetonitrile and 0.1% formic acid/75% acetonitrile sequentially, separated by an analytical capillary column (50 μm × 10 cm) packed with 5 μm spherical C18 reversed phase material (YMC, Kyoyo, Japan). A Waters nanoAcquity UPLC system (Waters, Milford, USA) was used to generate the following HPLC gradient: 0-30% B in 40 min, 30-70% B in 15 min (A = 0.1% formic acid in water, B = 0.1% formic acid in acetonitrile). The eluted peptides were sprayed into a LTQ Orbitrap Velos mass spectrometer (ThermoFisher Scientific, San Jose, CA, USA) equipped with a nano-ESI ion source. The mass spectrometer was operated in data-dependent mode with one MS scan followed by four CID (Collision Induced Dissociation) and four HCD (High-energy Collisional Dissociation) MS/MS

scans for each cycle. Database searches were performed on an in-house Mascot server (Matrix Science Ltd., London, UK) against Brassinazole-Resistant 2 (BZR2/BES1) protein sequence. All identified phosphorylated peptides were manually checked to exclude false-positives.

Materials and Methods S4 Primers used in this study

HIS-BES1-F: 5’-ACAGAATTCATGACGTCTGACGGAGC-3’

HIS-BES1-R: 5’-ACAGCGGCCGCTCAACTATGAGCTTTACCATTTC-3’

BES1-PROMOTER-F: 5’-ACTGGTACCTGGGCGCATTCCCTAGGGTG-3’

BES1-FLAG-F: 5’-ACAGGTACCATGACGTCTGACGGAGC-3’

BES1-FLAG-R: 5’-ACATTCGAAACTATGAGCTTTACCATTTC-3’

$BES1^{S137A}$-F: 5’-TCTTCTTCATTCCCGGCTCCTTCTCGAGTTGG-3’

$BES1^{S137A}$-R: 5’-CCAACTCGAGAAGGAGCCGGGAATGAAGAAGA-3’

$BES1^{S286A}$-F: 5’-GCACCACAGCAATTGGCTCCAAACACAGCAG-3’

$BES1^{S286A}$-R: 5’-CTGCTGTGTTTGGAGCCAATTGCTGTGGTGC-3’

$MKK5^{K99M}$-F: 5’-ACGTCCTTTCGCTCTCATGGTGATTTACGGAAAC-3’

$MKK5^{K99M}$-R: 5’-GTTTCCGTAAATCACCATGAGAGCGAAAGGACGT-3’

$MPK6^{AEF}$-F: 5’-GAGAGTGATTTCATGGCTGAATTTGTTGTCACGAGATG-3’

$MPK6^{AEF}$-R: 5’-CATCTCGTGACAACAAATTCAGCCATGAAATCACTCTC-3’

MPK6-BamHI-F: 5’-AGAGGATCCAATGGACGGTGGTTCAG-3’

MPK6-SalI-R: 5’-TCTGTCGACCTATTGCTGATATTCT-3’

BIK1-KpnI-F: 5’-AGCGGTACCTCAGCTCAAGCAGCTGAAG-3’

BIK1-SalI-R: 5’-TTAGTCGACCACAAGGTGCCTGCCAAAAG-3’

TUBLIN-RT-F: 5’-TGCCTTGAATGTTGATGTGACTGAG-3’

TUBLIN-RT-R: 5’-TCATCATCCTCATCGTCACCACCTT-3’

BES1-RT-F: 5’-AGCTGCAGCAGCAGCGATG-3’

BES1-RT-R: 5’-AGATATTGTGTGGATCAC-3’

$MPK6^{KM}$-F: 5’-GAGAGCGTTGCGATTAGAAGAATTGCTAACGCTTTTG-3’

$MPK6^{KM}$-R: 5’-CAAAAGCGTTAGCAATTCTTCTAATCGCAACGCTCTC-3’

WRKY22-RT-F: 5’-AAGCTCATCAGCTACTACC-3’

WRKY22-RT-R: 5’-CTAGAGGTATTGGAGCCAC-3’

FRK1-RT-F: 5’-TCTGAAGAATCAGCTCAAGGC-3’

FRK1-RT-R: 5’-TGTTGGCTTCACATCTCTGTG-3’

PRE1-RT-F: 5’-GTTCTGATAAGGCATCAGCCTCG-3’

PRE1-RT-R: 5’-CATGAGTAGGCTTCTAATAACGG-3’

PRE5-RT-F: 5’- AACGGCGTCGTTCTGATAAG-3’

PRE5-RT-R: 5’-CATGAGTAAGCTTCTAATCACGG-3’

CPD-RT-F: 5’-TTGCTCAACTCAAGGAAGAG-3’

CPD-RT-R: 5’-TGATGTTAGCCACTCGTAGC-3’

BR6OX2-RT-F: 5’-AAACCAAAGACTAAGATATGGGG-3’

BR6OX2 -RT-R: 5’-GAATATCAAGCATAGATTGCGG-3’

BZR1-RT-F: 5’-GCAGATGTCTCCAAATACTGCTGCCT-3’

BZR1-RT-R: 5’-GACATGCCATTTGGGTTTGCCTAG-3’

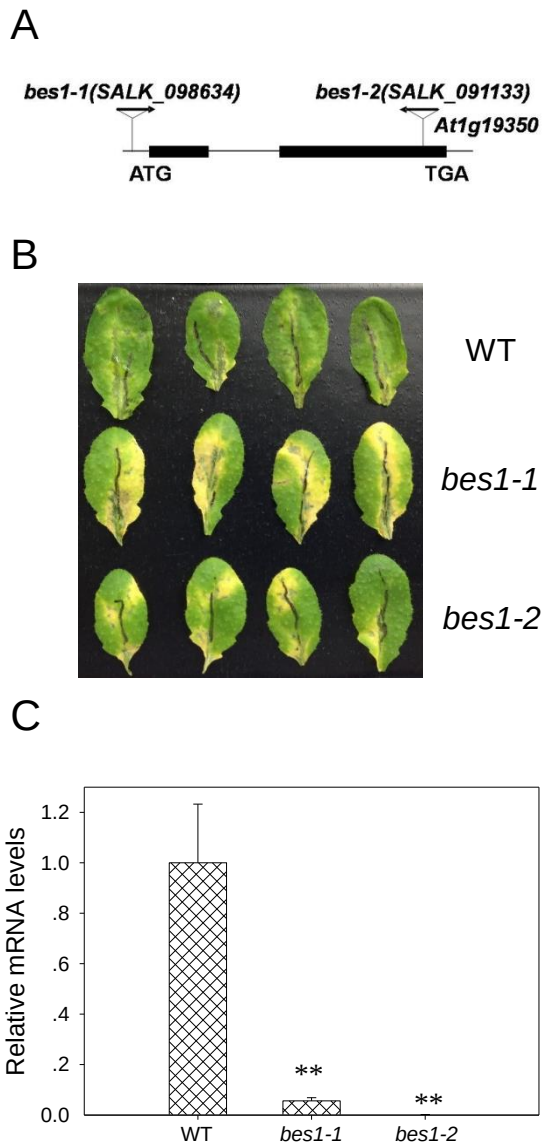

Figure S1. Characterization and disease symptom of *bes1-1* and *bes1-2* mutants.
A, Schematic presentation of T-DNA insertions in *BES1*. Boxes denote predicated open reading frames. Inverted triangle indicates position of T-DNA insertion. B, Disease symptom of 5-week-old WT, *bes1-1* and *bes1-2* plant leaves. Leaves infiltrated with 10^6 CFU ml^{-1} *Pst* DC3000 were photographed 3 days post inoculation. C, Quantitative RT-PCR analysis of *BES1* transcript levels in *bes1-1* and *bes1-2* mutants. Total RNA of 5-week-old plants was extracted and used for reverse transcription. Real-Time PCR was performed following standard protocols. Values are normalized to *TUBLIN* control. Error bars indicate standard deviation of 3 technical repeats. ** indicates significant difference at *P* value <0.01. Similar results were observed in 3 independent biological repeats.

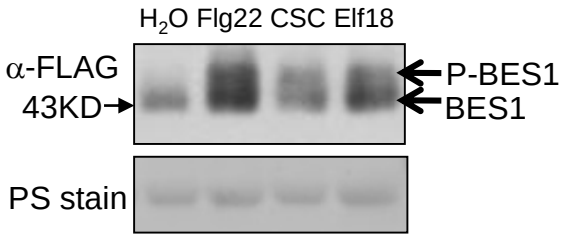

Figure S2. Chitin and Elf18 induce BES1 phosphorylation.
CSC (Crab shell chitin) and Elf18 (an *N*-acetylated peptide comprising the first 18 amino acids of EF-Tu) induce BES1 phosphorylation in protoplasts. Col-0 protoplasts were transfected with *35S::BES1-FLAG*, treated with 1 μM flg22, 200 mg ml^{-1} csc or 1 μM elf18 respectively for 5 minutes. Total proteins extracted from protoplasts were separated by SDS-PAGE and subjected to anti-FLAG immunoblot. Ponceau S (PS) staining of the filter indicates loading of the protein.

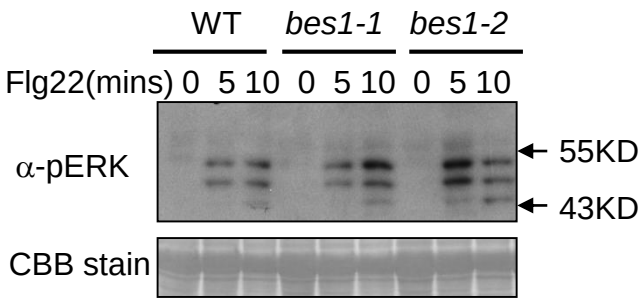

Figure S3. Normal flg22-induced MAPK activation in *bes1-1* and *bes1-2* mutants.
Flg22 induces comparable MAPK activation in *bes1-1, bes1-2* and WT plants. WT and mutant plants were sprayed with 10 μM flg22 or H_2O for the indicated time. Protein samples were separated by SDS-PAGE and subjected to anti-pERK immunoblot. CBB staining of the filter indicates loading of the protein. .

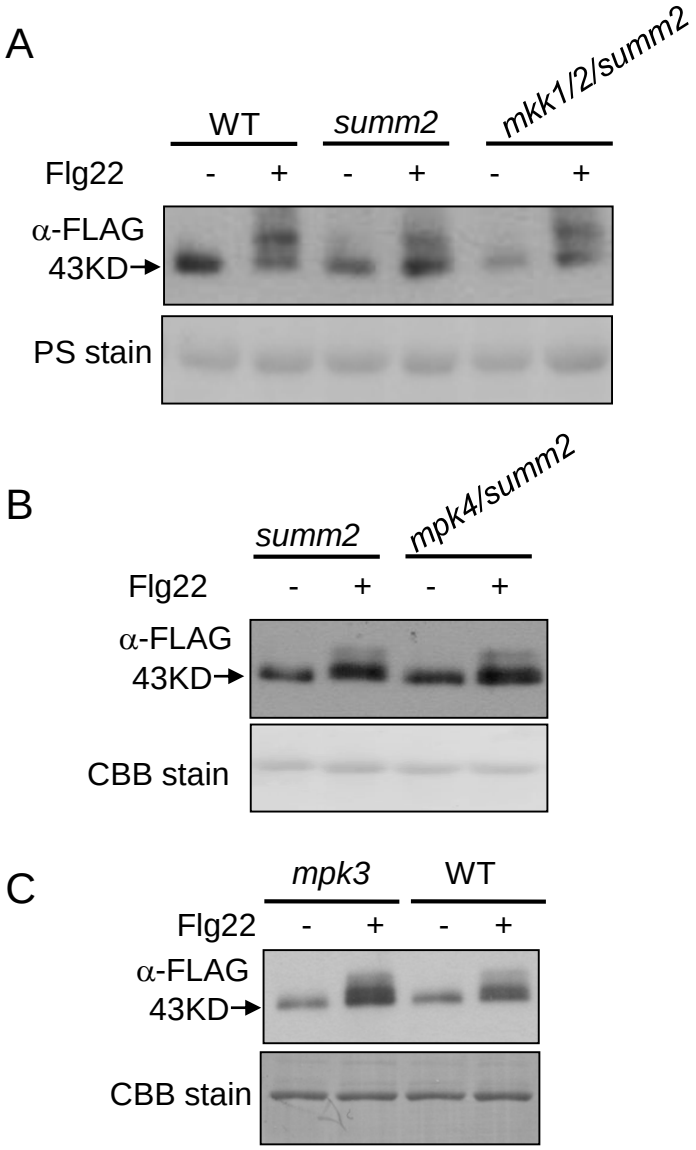

Figure S4. Mutation of *MPK4*, *MKK1/2* or *MPK3* is not sufficient to block flg22-induced BES1 phosphorylation.

A, BES1 phosphorylation induced by flg22 in *mkk1/mkk2/summ2* mutant. **B**, BES1 phosphorylation induced by flg22 in *mpk4/summ2* mutant. Protoplasts isolated from WT, *summ2*, *mpk4/summ2* or *mkk1/mkk2/summ2* mutant were transfected with *35S::BES1-FLAG*, treated with or without flg22. C, BES1 phosphorylation induced by flg22 in *mpk3* mutant. Col-0 and *mpk3* mutant protoplasts were transfected with *35S::BES1-FLAG*, treated with or without 1 μM flg22. Protein samples were separated by SDS-PAGE and subjected to anti-FLAG immunoblot. PS or CBB staining of the filter indicates loading of the protein.

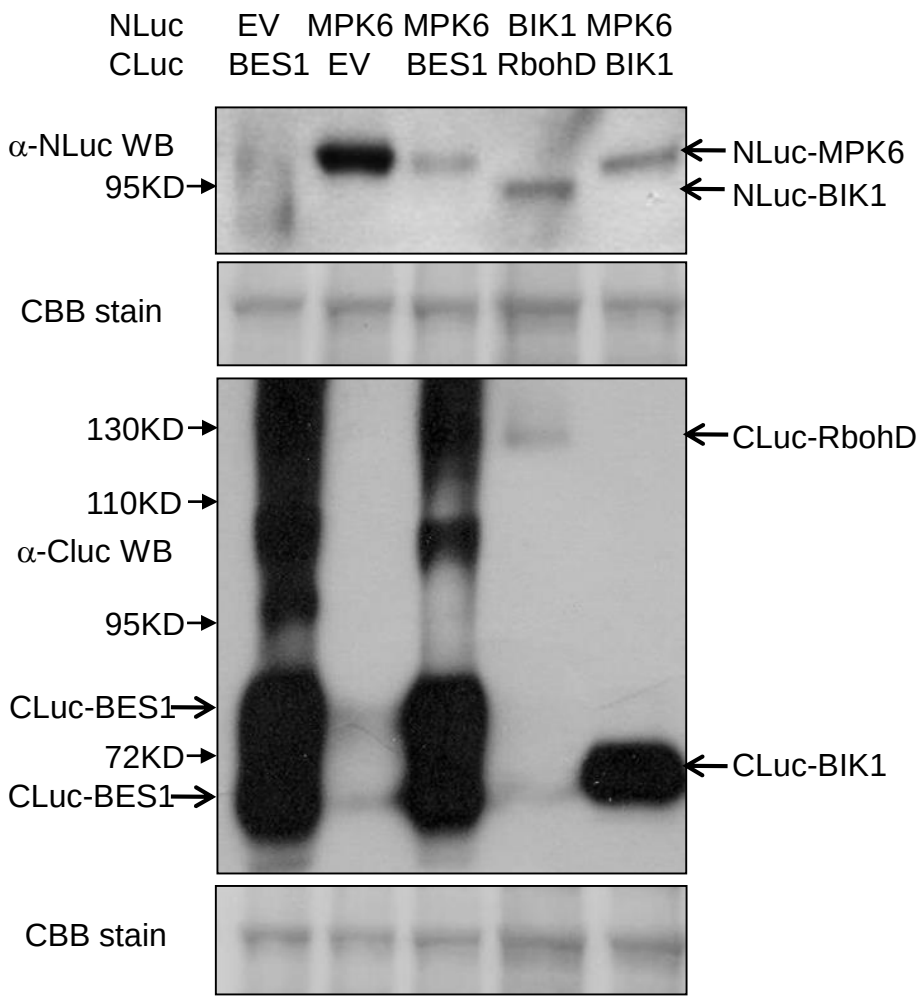

Figure S5. Expression levels of NLuc- and CLuc-fusion proteins in *Nicotiana benthamiana*. A, NLuc-fusion proteins was detected by anti-Luc immune-blot. B, CLuc-fusion proteins was detected by anti-CLuc immune-blot. CBB staining of the filter indicates loading of the protein.

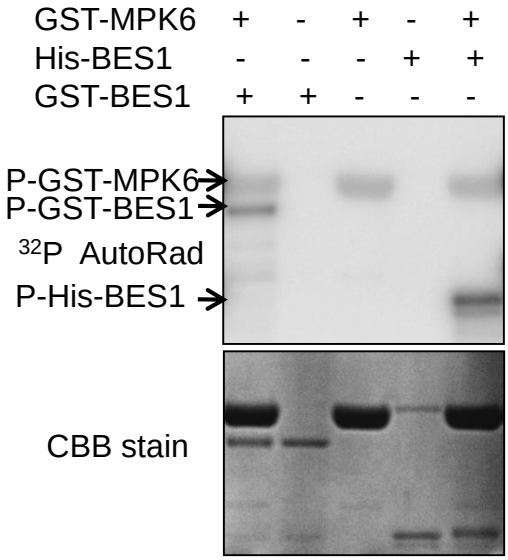

Figure S6. BES1 is phosphorylated by MPK6 *in vitro*.
GST-BES1 or His-BES1 was incubated with GST-MPK6 and subjected to *in vitro* phosphorylation assay. CBB staining indicates loading of the protein.

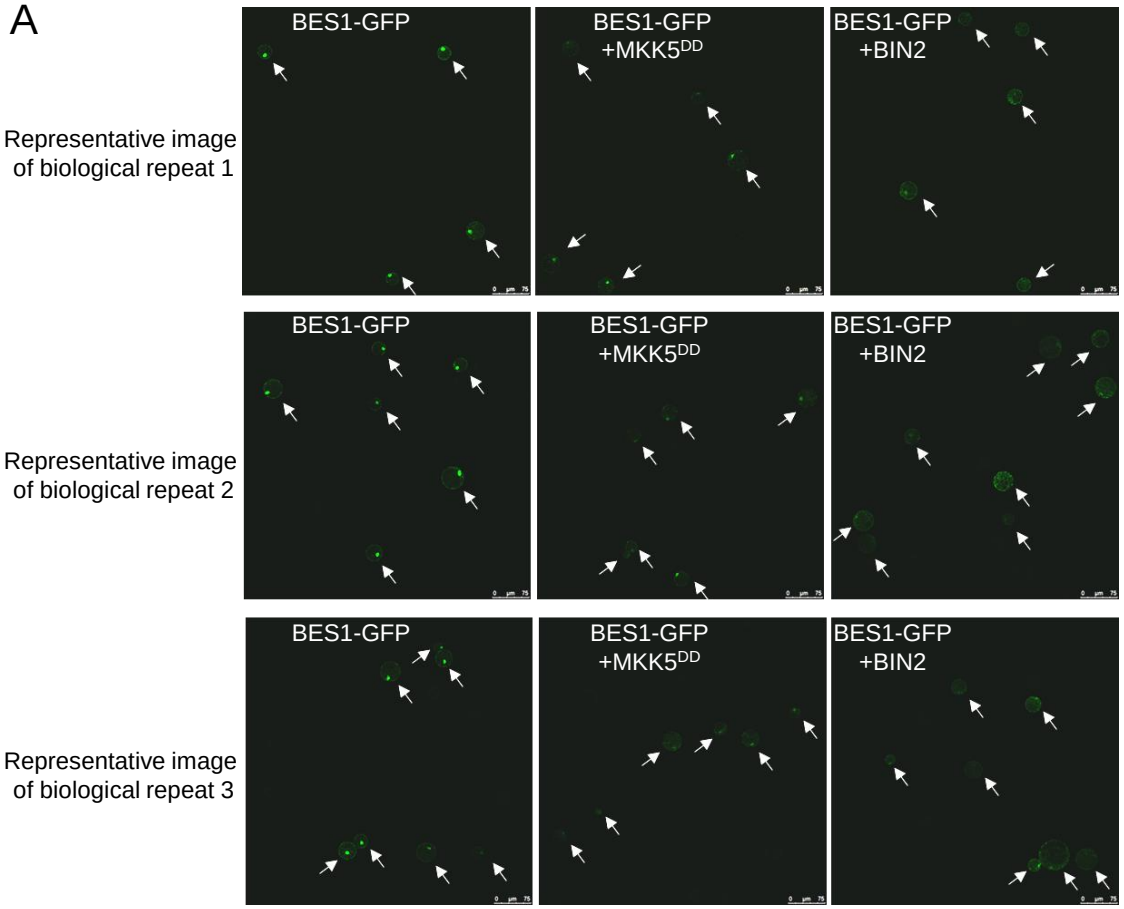

Figure S7. Co-expression of MKK5^{DD} reduced nucleus accumulation of BES1-GFP in Arabidopsis protoplasts.

A, Representative confocal image of BES1-GFP subcellular accumulation. GFP-fluorescent cells were indicated by arrows. B, Quantitative relative nucleus to cytoplasm ratio of BES1-GFP. Protoplasts were transfected with *35S::BES1-GFP* alone, or together with *35S::MKK5* or *35S::BIN2* as indicated. The subcellular locations of BES1-GFP were examined using Leica SP8 confocal microscopy 8 hours after transfection. The intensities of the nucleus and cytoplasm fluorescent signals of 30 cells in each treatment was determined by Leica LAS AF Lite software. Data are means ± SE (n = 30). ** indicates significant difference at *P* value <0.01. Similar results were observed in 3 independent biological repeats.

A

Potential phosphorylation sites phosphorylated by MPK6 activated by MKK5^{DD}	
Peptide Sequence identified	**Modification**
KGHKPLPGDMAGp(SSS)R	1phospho
GHKPLPGDMAGp(SSS)R	1phospho
ATPYSSHNQSPLSSTFDSPILSYQVSPSSp(SSFPSPS)R	1phospho
ApTPYSSHNQSPLSSTFDpSPILSYQVSPSSSSFPSPSR	2phospho
ApTPYSSHNQSPLSSTFDpSPILSYQVSPSSSSFPpSPSR	3phospho
SSHNQSPLSSTFDSPILSYQVSPSSp(SSFPSPS)R	1phospho
SHNQSPLSSTFDSPILpSYQVSPSSSSFPpSPSR	2phospho
pSHNQSPLSSTFDSPILpSYQVSPSSSSFPpSPSR	3phospho
QVpSPSSSSFPSPpSR.	2phospho
QVSPSSSpSFPpSPSR.	2phospho
VGDPHNIp(ST)IFPFLR	1phospho
NISpTIFPFLR	1phospho
NGGIPp(SS)LPPLR	1phospho
NPKPLPpTWESFTK	1phospho
PLPTWEpSFTK	1phospho
LVKPAPQQLpSPNTAAIQEIGQSSEFK	1phospho
PAPQQLpSPNTAAIQEIGQSSEFK	1phospho
PAPQQLSPNpTAAIQEIGQSSEFK	1phospho
Note 1: Serine 137 or Serine 286 residue was shown in red.	
Note 2: Peptide containg serine residues followed immediately by proline are hilighted in yellow.	

B

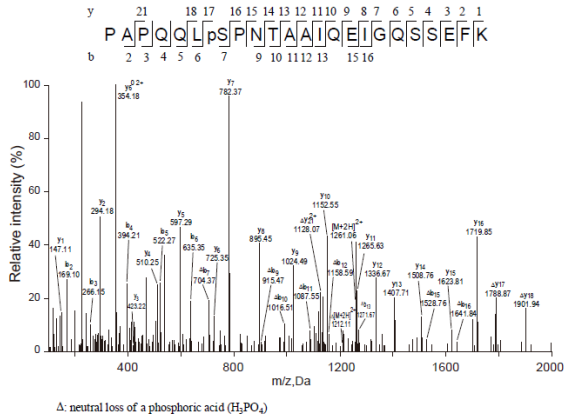

C

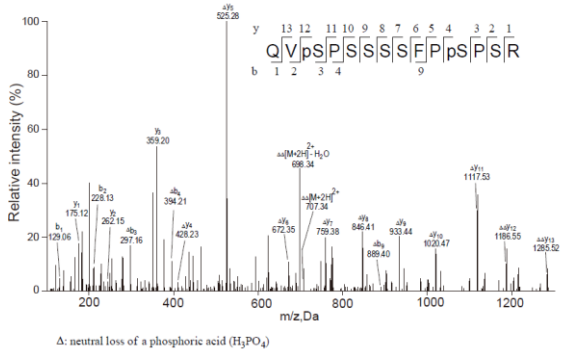

Figure S8. Mass spectrometry analysis of BES1 phosphorylation sites.

A, Peptide sequences containing potential phosphorylation sites phosphorylated by MPK6 activated by MKK5^{DD}. p indicates phosphorylation of the following residue. B, Mass spectrometry analysis of S286 residue. C, Mass spectrometry analysis of S137 and S129 residues.

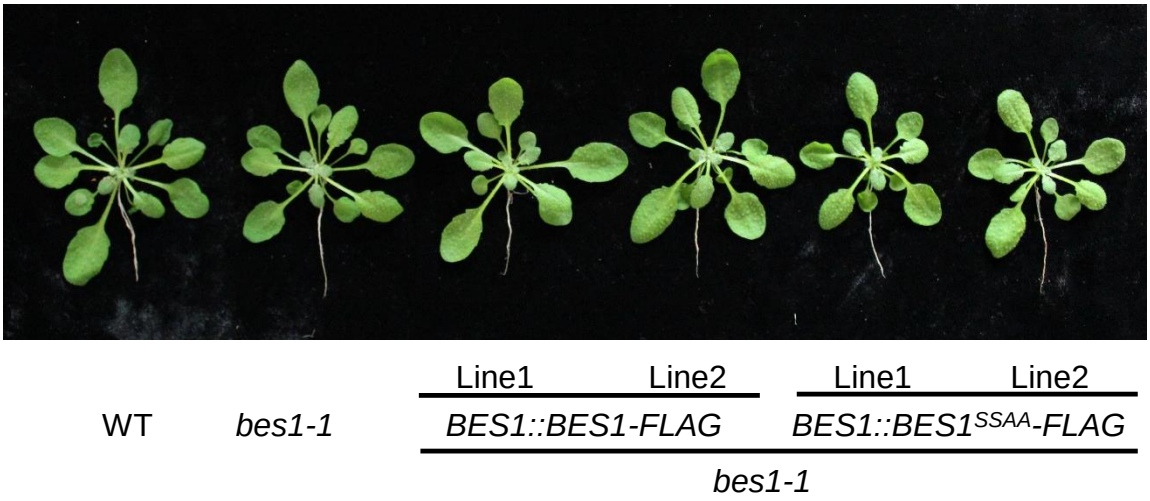

Figure S9. Morphologic phenotype of *bes1-1*, *bes1-1*/*BES1::BES1-FLAG* and *bes1-1*/*BES1::BES1^{SSAA}-FLAG* plants.

5-week-old WT, *bes1-1*, *bes1-1*/*BES1::BES1-FLAG* and *bes1-1*/*BES1::BES1^{SSAA}-FLAG* plants grown under short-day conditions were photographed.

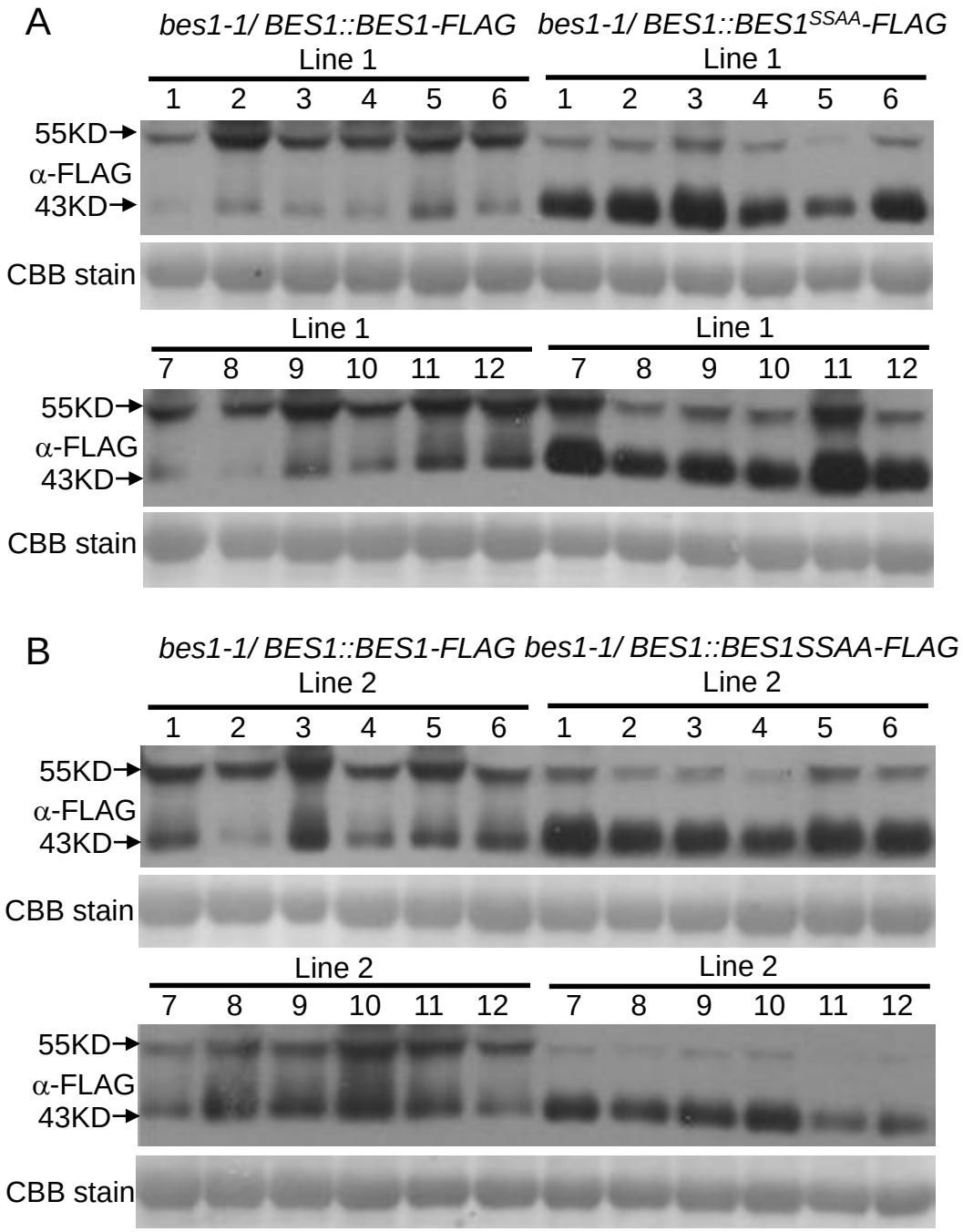

Figure S10. Expression levels of BES1-FLAG and BES1^{SSAA}-FLAG in *bes1-1*/ *BES1::BES1-FLAG* and *bes1-1*/ *BES1::BES1^{SSAA}-FLAG* plants.

Transgenic seeds carrying GFP fluorescence in seed oil body membrane were selected and then used for the experiments in this study. The expression levels of the transgenes was further confirmed by western blot. Total protein extracted from leaves was separated by SDS-PAGE and subjected to anti-FLAG immunoblot. CBB staining of the filter indicates loading of the protein. Results shown are representative of transgene expression in *bes1*/*BES1::BES1-FLAG* and *bes1*/*BES1::BES1^{SSAA}-FLAG* line 1 (A) and line 2 (B) transgenic lines.

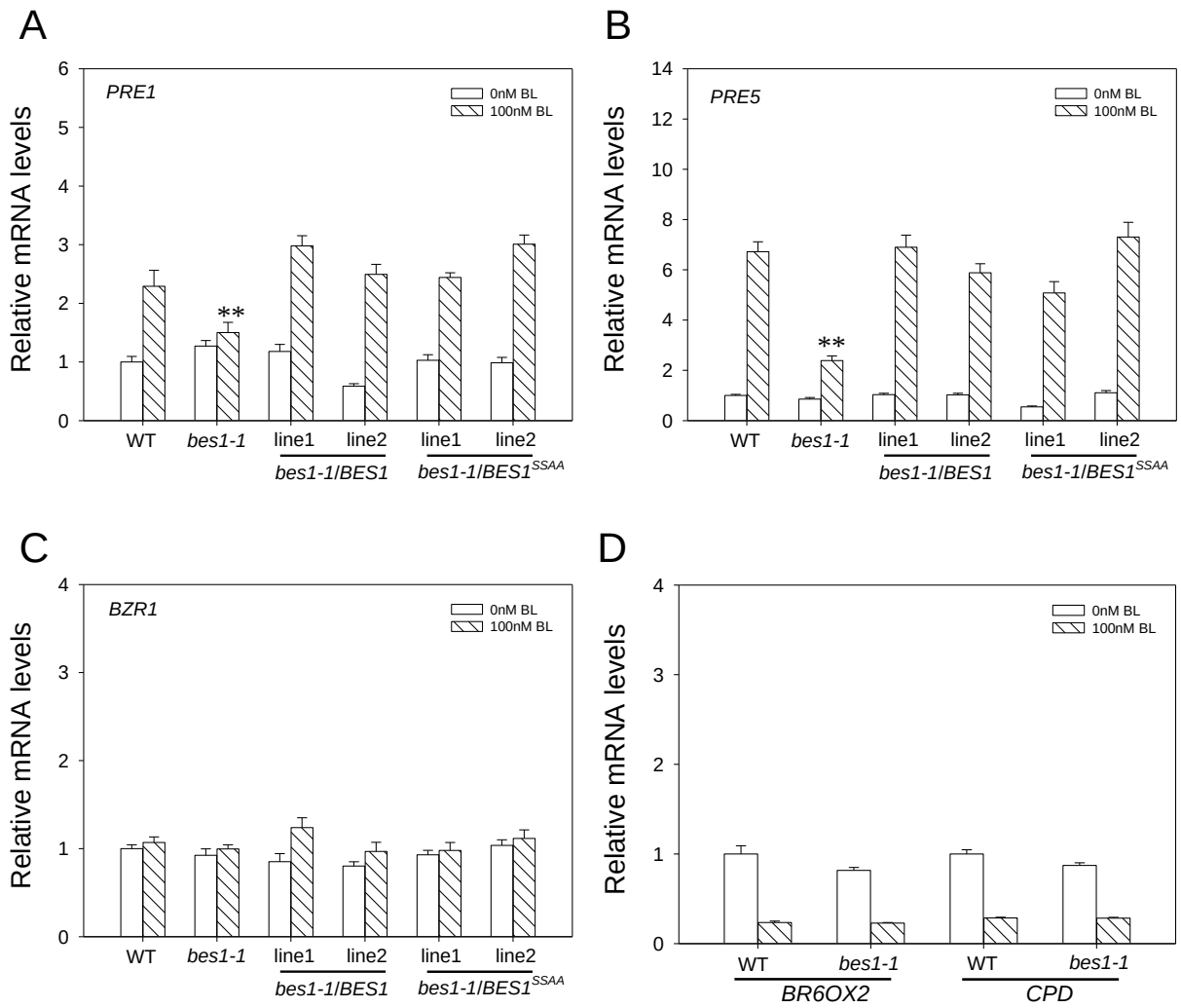

Figure S11. BES1 S286 and S137 are not required for the induction of *PRE1* and *PRE5* by epiBL.

5-week-old WT, *bes1-1*, *bes1*/*BES1::BES1-FLAG* and *bes1*/*BES1::BES1*^{SSAA}*-FLAG* plants were treated with or without 100 nM epiBL for 3 hours. Expression of *PRE1* (A), *PRE5* (B), *BZR1* (C), *BR6OX2* and *CPD* (D) was measured by Real-Time PCR. Total RNA from leaves was extracted and used for reverse transcription. Real-Time PCR was performed following standard protocols. Values are normalized to *TUBLIN* control and are presented as relative to the value of 0nM epiBL-treated WT plants. Error bars indicate standard deviation of 3 technical repeats. ** indicates significant difference to 100nM epiBL-treated WT plants at *P* value <0.01. Similar results were observed in 3 independent biological repeats.

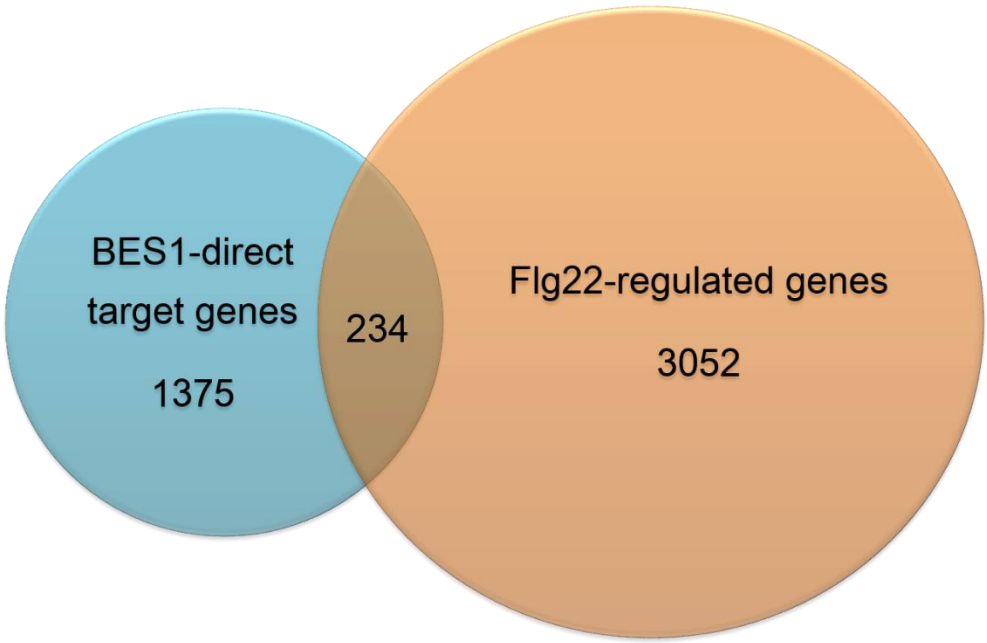

Figure S12. A comparison of BES1-direct target genes (Yu et al., 2011) with flg22-regulated genes (Chen et al., 2009).

Venn diagram shows overlaps among BES1-direct target genes and flg22-regulated genes.